Supplementary Information

Supplementary Results: synthesis and characterization of new endoperoxides.

General.

The incorporation of an oxygen atom into the organic frameworks from atmospheric molecular oxygen (O_2) offers one of the most ideal processes in organic synthesis.[1,2] We have recently developed the Cu-catalyzed benzylic methylene C-H oxygenation (carbonylation) under an O_2 atmosphere via the *N*-H imine intermediate, which could be generated from the reaction of carbonitriles and Grignard reagents.[3] During the course of this study, we also found that the present aerobic reaction of 2-cyclohexylbenzonitrile bearing a tertiary benzylic C-H bond with *p*-tolylmagnesium bromide afforded a very stable novel crystal compound, benzo[*d*][1,2]dioxin-1-amine (amino endoperoxide) (4-Me), in 70% yield via tertiary C-H oxygenation followed by intramolecular cyclization of the resulting peroxide moiety (entry 1). This concise one-pot synthesis of the novel amino endoperoxide prompted us to investigate its scope and limitations. Various aryl Grignard reagents could be utilized for synthesis of the corresponding amino endoperoxides in good yields regardless of the electron density and bulkiness of the benzene ring introduced. Moreover, the amine moiety of the amino endoperoxide (4-Me) could be converted into azido and hydroxyl groups by treating 4-Me with t-BuONO and the corresponding nucleophiles ($TMSN_3$ or H_2O), keeping the endoperoxide structure intact (for N_3 and OH, entries 13 and 14, Figure 1). The synthetic procedures and spectral data were described below (pages 2-40 of Supplementary Information). The structures of these endoperoxides except for 4-OMe (entry 5) and 4-F (entry 7) were secured by X-ray crystallographic analysis.

^{1}H NMR (400 MHz) spectra were recorded on a Bruker Avance 400 spectrometer in $CDCl_3$ [using TMS (for ^{1}H, $\delta = 0.00$) as internal standard]. ^{13}C NMR (100 MHz) spectra on a Bruker Avance 400 spectrometer in $CDCl_3$ [using $CDCl_3$ (for ^{13}C, $\delta = 77.23$) as internal standard]. The following abbreviations were used to explain the multiplicities: s = singlet, d = doublet, t = triplet, q = quartet, br = broad. IR spectra were recorded on a Shimazu IR IRAffinity-1 FT-IR Spectrometer. High-resolution mass spectra were obtained with a Finnigan MAT 95 XP mass spectrometer (Thermo Electron Corporation). Melting points are uncorrected and were recorded on a MPA 100 OptiMelt Automated Melting Point System. Flash chromatography was performed using Merck silica gel 60 with distilled solvents. Anhydrous DMF was purchased from Sigma-Aldrich and used as received. All Grignard reagents were freshly prepared from the corresponding arylbromides and magnesium in Et_2O, titrated, and stored under N_2 atmosphere at 0 °C.

Typical Procedure for Synthesis of Amino Endoperoxides

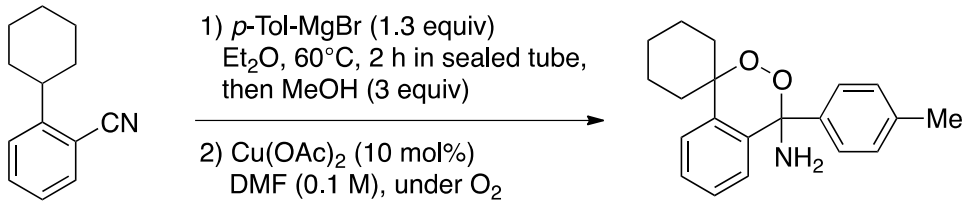

1

To a solution of 2-cyclohexylbenzonitrile[4] (92.6 mg, 0.500 mmol) in Et_2O (0.5 mL) was added an Et_2O solution of *p*-tolylmagnesium bromide (1.3 equiv). The reaction mixture was stirred at 60 °C in a sealed tube for 2 h. Anhydrous MeOH (50 µL, 3 equiv) was then added. $Cu(OAc)_2$ (91 mg, 10 mol%) and anhydrous DMF (5 mL) was then added. The reaction mixture was stirred at 80 °C under an O_2 atmosphere for 8.5 h. The reaction was quenched with pH 9 buffer solution and extracted three times with Et_2O (20 mL). The combined organic extracts were washed with water and brine. After drying with $MgSO_4$, the solvents were removed under reduced pressure. The resulting crude material were purified by flash column chromatography (hexane : ethyl acetate = 9 : 1) to afford 4-(*p*-tolyl)-4*H*-spiro[benzo[*d*][1,2]dioxine-1,1'-cyclohexan]-4-amine (**1**) (108 mg, 0.35 mmol) in 70 % yield.

Compound Data
4-(*p*-tolyl)-4*H*-spiro[benzo[*d*][1,2]dioxine-1,1'-cyclohexan]-4-amine, (1) 4-Me

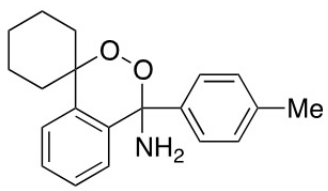

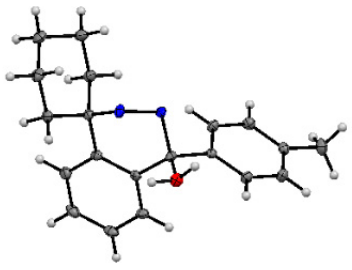

White granular crystal (CCDC 806338); mp. 140.8-141.0 °C; IR (NaCl) 3682, 2938, 2860, 1732, 1510, 1447, 1425 cm^{-1}; ^{1}H NMR (400 MHz, $CDCl_3$) δ 1.27-1.40 (1H, m), 1.64-1.83 (7H, m), 1.94-1.98 (2H, m), 2.32 (3H, s), 2.72 (2H, br), 7.09-7.14 (4H, m), 7.17 (1H, d, *J* = 7.6 Hz), 7.21-7.23 (1H, m), 7.40 (2H, d, *J* = 8.0 Hz); ^{13}C NMR (100 MHz, $CDCl_3$) δ 21.1, 21.5, 21.8, 25.4, 35.0, 35.4, 81.1, 82.2, 123.5, 126.3, 126.9, 127.3, 128.2, 128.8, 137.3, 138.2 (overlapped), 140.9; ESIHRMS: Found: m/z 310.1800. Calcd for $C_{20}H_{24}NO_2$: $(M+H)^+$ 310.1807.

4-phenyl-4*H*-spiro[benzo[*d*][1,2]dioxine-1,1'-cyclohexan]-4-amine, (2) H

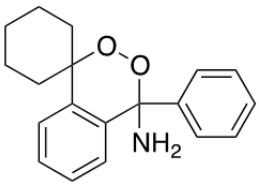

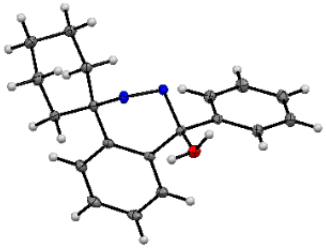

70% yield from 2-cyclohexylbenzonitrile and phenylmagnesium bromide; Colorless crystals (CCDC 891329); mp. 161.8-162.3 °C; IR (ATR) 3383 3321 3312 1260 1244 cm^{-1}; ^{1}H NMR (400 MHz, $CDCl_3$) δ 1.49 – 1.27 (1H, m), 1.86 – 1.55 (6H, m), 1.95 (2H, br), 2.42 (1H, br), 2.72 (2H, br), 7.42 – 6.98 (7H, m), 7.64 – 7.45 (2H, m); ^{13}C NMR (100 MHz, $CDCl_3$) δ 21.8, 22.0, 25.7, 35.3, 35.6, 81.4, 92.5, 123.8, 126.5, 127.2, 127.6, 128.4, 128.5 (overlapped), 128.6, 137.4, 141.1; EIHRMS: Found: *m/z* 296.1660. Calcd for $C_{19}H_{22}NO_2$: $(M+H)^+$ 296.1651.

4-(4-(trifluoromethyl)phenyl)-4*H*-spiro[benzo[*d*][1,2]dioxine-1,1'-cyclohexan]-4-amine, (3) 4-CF_3

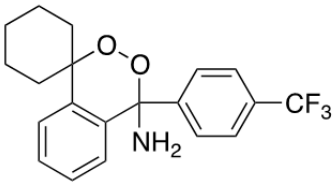

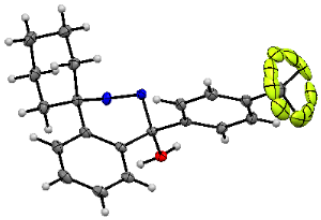

70% yield from 2-cyclohexylbenzonitrile and (4-trifluoromethylphenyl)magnesium bromide; Colorless Crystals (CCDC 891331); mp. 143.4-145.9 °C; IR (ATR) 3393 3331 1321 831 cm^{-1}; ^{1}H NMR (400 MHz, $CDCl_3$) δ 1.49 – 1.26 (1H, m), 1.88 – 1.61 (6H, m), 2.01 (2H, br), 2.32 (1H, br), 2.69 (2H, br), 7.34 – 6.99 (2H, m), 7.64 – 7.53 (4H, m), 7.69 (2H, d, *J* = 8.3 Hz); ^{13}C NMR (100 MHz, $CDCl_3$) δ 21.8, 21.9, 25.6, 35.4, 35.6, 81.6, 92.2, 124.3 (q, $J_{C\text{-}F}$ = 270.4 Hz), 124.2, 125.4 (q, $J_{C\text{-}F}$ = 3.8 Hz), 126.7, 127.7, 128.1, 128.2, 130.7 (q, $J_{C\text{-}F}$ = 32.3 Hz), 136.5, 141.2, 145.7; EIHRMS: Found: *m/z* 364.1524. Calcd for $C_{20}H_{21}NO_2F_3$: $(M+H)^+$ 364.1524.

4-(2-methoxyphenyl)-4*H*-spiro[benzo[*d*][1,2]dioxine-1,1'-cyclohexan]-4-amine, (4) 2-OMe

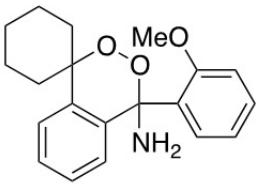

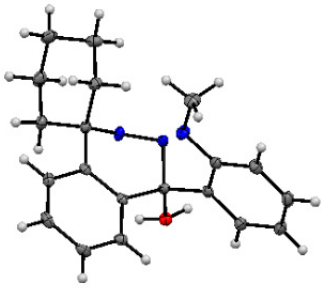

68% yield from 2-cyclohexylbenzonitrile and (2-methoxyphenyl)magnesium bromide; Colorless Crystals (CCDC 891333); mp. 133.0-134.1 °C; IR (ATR) 3566 1489 1244 1026 cm^{-1}; ^{1}H NMR (400 MHz, $CDCl_3$) δ 1.39 – 1.09 (1H, m), 1.94 – 1.39 (7H, m), 2.15 (2H, br), 3.01 (2H, br), 3.81 (3H, br), 6.80 (1H, br), 6.94 (2H, br), 7.85 – 7.06 (5H, m); ^{13}C NMR (100 MHz, $CDCl_3$) δ 21.7, 21.9, 25.7, 34.8, 35.5, 55.8, 81.2, 93.4, 112.3, 120.1, 123.9, 126.3 (overlapped), 127.6, 127.7, 129.9, 131.2, 137.5, 142.3, 158.0; EIHRMS: Found: *m/z* 326.1767. Calcd for $C_{20}H_{24}NO_3$: $(M+H)^+$ 326.1756.

4-(4-methoxyphenyl)-4*H*-spiro[benzo[*d*][1,2]dioxine-1,1'-cyclohexan]-4-amine, (5) 4-OMe

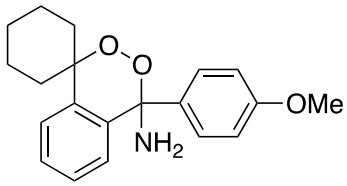

74% yield from 2-cyclohexylbenzonitrile and (4-methoxyphenyl)magnesium bromide; Colorless Solids; mp. 191.8-192.2 °C; IR (ATR) 3647 1508 1240 1032 cm^{-1}; ^{1}H NMR (400 MHz, $CDCl_3$) δ 1.44 – 1.28 (1H, m), 2.12 – 1.52 (8H, m), 2.44 (1H, br), 2.71 (2H, br), 3.76 (3H, s), 6.90 – 6.79 (2H, m), 7.15 – 6.98 (2H, m), 7.29 – 7.15 (2H, m), 7.51 – 7.40 (2H, m); ^{13}C NMR (100 MHz, $CDCl_3$) δ 21.8, 22.0, 25.7, 35.2, 35.7, 55.4, 81.4, 92.3, 113.7 (overlapped), 123.8, 126.5, 127.6, 128.5, 128.6, 137.7, 141.1, 159.8; EIHRMS: Found: *m/z* 326.1754. Calcd for $C_{20}H_{24}NO_3$: $(M+H)^+$ 326.1756.

4-(4-chlorophenyl)-4*H*-spiro[benzo[*d*][1,2]dioxine-1,1'-cyclohexan]-4-amine, (6) 4-Cl

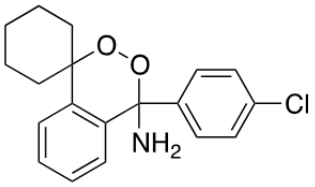

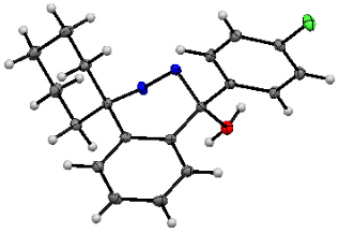

67% yield from 2-cyclohexylbenzonitrile and (4-chlorophenyl)magnesium bromide; Colorless Crystals (CCDC 891335), mp. 163.5-164.3 °C; IR (ATR) 3379, 3308, 1558, 1142, 1090 cm^{-1}; 1H NMR (500 MHz, CDCl3) δ 1.44 – 1.28 (1H, m), 1.87 – 1.60 (7H, m), 2.00 (1H, br), 2.36 (1H, br), 2.67 (2H, br), 7.11 (1H, m), 7.22 – 7.17 (1H, m), 7.35 – 7.22 (4H, m), 7.48 (2H, d, *J* = 8.6 Hz); ^{13}C NMR (100 MHz, $CDCl_3$) δ

21.5, 21.7, 25.4, 35.1, 35.4, 81.3, 91.9, 123.8, 126.4, 127.6, 127.7, 128.0, 128.3, 128.3, 128.5, 134.3, 136.6; EIHRMS: Found: *m/z* 330.1265. Calcd for $C_{19}H_{21}NO_2Cl$: $(M+H)^+$ 330.1261.

4-(4-fluorophenyl)-4*H*-spiro[benzo[*d*][1,2]dioxine-1,1'-cyclohexan]-4-amine, (7) 4-F

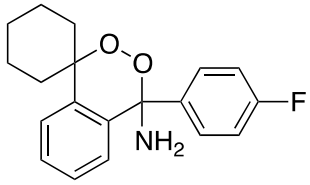

70% yield from 2-cyclohexylbenzonitrile and (4-fluorophenyl)magnesium bromide; Colorless Solids; mp. 161.7-163.1 °C; IR (ATR) 3566 3524 1522 1506 1221 cm^{-1}; ^1H NMR (400 MHz, $CDCl_3$) δ 1.46 – 1.19 (1H, m), 1.89 – 1.46 (7H, m), 1.94 (2H, br), 2.38 (1H, br), 2.69 (2H, br), 7.31 – 6.93 (8H, m), 7.57 – 7.44 (2H, m); ^{13}C NMR (100 MHz, $CDCl_3$) δ 21.7, 22.0, 25.6, 35.3, 35.6, 81.4, 92.1, 115.2 (*d*, J_{C-F} = 21.1 Hz), 123.9, 126.6, 127.8, 128.3, 129.1, 129.2, 137.2, 141.0, 162.9 (*d*, J_{C-F} = 245.8 Hz); EIHRMS: Found: *m/z* 314.1552. Calcd for $C_{19}H_{21}NO_2F$: $(M+H)^+$ 314.1556.

4-(3-chlorophenyl)-4*H*-spiro[benzo[*d*][1,2]dioxine-1,1'-cyclohexan]-4-amine, (8) 3-Cl

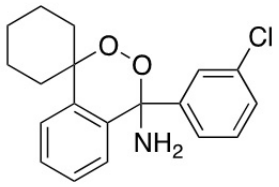

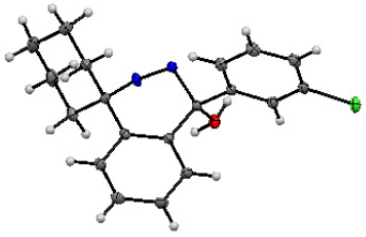

61% yield from 2-cyclohexylbenzonitrile and (3-chlorophenyl)magnesium bromide; Colorless Crystals (CCDC 891337); mp. 149.7-150.3°C; IR (ATR) 3395, 3318, 1595, 1159,1142, 1132, 1076 cm^{-1}; ^1H NMR (400 MHz, $CDCl_3$) δ 1.47 – 1.25 (1H, m), 1.88 – 1.59 (7H, m), 1.95 (2H, br), 2.26 (1H, br), 2.66 (2H, br), 7.17 – 7.03 (2H, m), 7.22 – 7.17 (1H, m), 7.33 – 7.22 (3H, m), 7.48 – 7.40 (1H, m), 7.56 (1H, d, *J* = 1.7 Hz); ^{13}C NMR (100 MHz, $CDCl_3$) δ 21.5, 21.7, 25.4, 35.1, 35.4, 81.3, 91.9, 123.8, 125.3, 126.4 (overlapped), 127.3, 127.7, 128.0, 128.6, 129.5, 134.2, 136.4, 140.9; EIHRMS: Found: *m/z* 330.1256. Calcd for $C_{19}H_{21}NO_2Cl$: $(M+H)^+$ 330.1261.

4-(naphthalen-1-yl)-4*H*-spiro[benzo[*d*][1,2]dioxine-1,1'-cyclohexan]-4-amine, (9) 1-Naphthyl

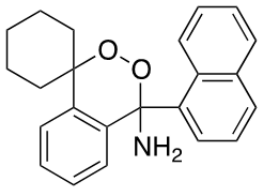

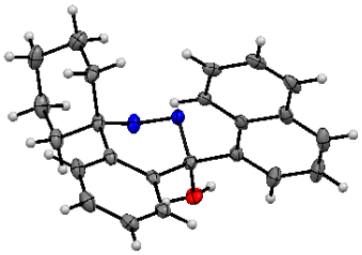

50% yield from 2-cyclohexylbenzonitrile and 1-naphthylmagnesium bromide; Pale Brown Crystals (CCDC 891339); mp. 166.5-166.9 °C; IR (ATR) 3566 3524 1522 1506 cm^{-1}; ^1H NMR (400 MHz, $CDCl_3$) δ 1.52 – 1.25 (1H, m), 1.98 – 1.64 (6H, m),

2.00 (1H, br), 2.14 (1H, br), 3.04 (2H, s), 7.08 (2H, br), 7.57 – 7.26 (6H, m), 7.87 (2H, dd, J = 11.7, 8.4 Hz), 8.04 (1H, br); ^{13}C NMR (100 MHz, $CDCl_3$) δ 21.9, 21.9 25.7, 35.0, 36.6, 81.7, 93.7, 124.7, 124.9, 125.4 (overlapped), 125.7, 126.7, 126.7, 127.4, 128.1, 129.0, 130.4, 130.8, 136.2, 138.1, 140.6; EIHRMS: Found: *m/z* 346.1815. Calcd for $C_{23}H_{24}NO_2$: $(M+H)^+$ 346.1807.

4-(naphthalen-2-yl)-4*H*-spiro[benzo[*d*][1,2]dioxine-1,1'-cyclohexan]-4-amine, (10) 2-Naphthyl

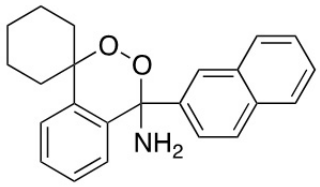

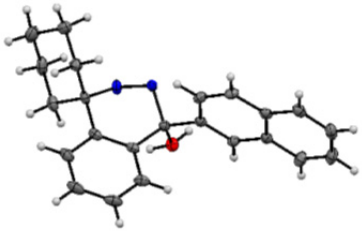

77% yield from 2-cyclohexylbenzonitrile and 2-naphthylmagnesium bromide; Colorless Crystals (CCDC 891341); mp. 178.8-179.9 °C; IR (ATR) 3588 3566 1558 1522 1506 cm^{-1}; ^{1}H NMR (400 MHz, $CDCl_3$) δ 1.47 – 1.14 (1H, m), 2.23 – 1.47 (9H, m), 2.49 (1H, br), 2.85 (2H, br), 7.32 – 6.86 (4H, m), 7.47 (3H, br), 8.00 – 7.59 (3H, m), 8.19 (1H, br); ^{13}C NMR (100 MHz, $CDCl_3$) δ 21.8, 22.1, 25.7, 35.4, 35.7, 81.6, 92.7, 124.0, 125.2, 126.4, 126.5, 126.6, 126.7, 127.8 (overlapped), 128.2, 128.6, 128.7, 133.1, 133.4, 137.2, 138.7, 141.2; EIHRMS: Found: *m/z* 346.1761. Calcd for $C_{23}H_{24}NO_2$: $(M+H)^+$ 346.1807.

4,4-dimethyl-1-(*p*-tolyl)-1,4-dihydrobenzo[*d*][1,2]dioxin-1-amine, (11) *di*-Me

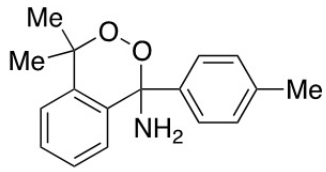

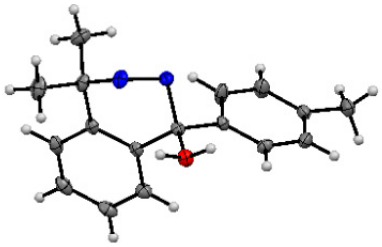

58% yield from 2-isopropylbenzonitrile[5] and *p*-tolylmagnesium bromide; Colorless Crystals (CCDC 891343); mp. 120.7-121.7 °C; IR (ATR) 3397, 3325, 1614, 1182, 1171 cm^{-1}; ^{1}H NMR (400 MHz, $CDCl_3$) δ 1.69 (3H, s), 2.32 (3H, s), 2.68 (2H, br), 7.19 – 7.07 (5H, m), 7.28 – 7.19 (1H, m), 7.53 – 7.33 (2H, m); ^{13}C NMR (100 MHz, $CDCl_3$) δ 21.1, 26.4, 27.7, 80.5, 92.3, 123.7, 126.4, 126.8, 127.5, 128.2, 128.9 (overlapped), 136.9, 138.2, 140.7; EIHRMS: Found: *m/z* 270.1490. Calcd for $C_{17}H_{20}NO_2$: $(M+H)^+$ 270.1494.

8-methoxy-4-(*p*-tolyl)-4*H*-spiro[benzo[*d*][1,2]dioxine-1,1'-cyclohexan]-4-amine, (12) 2'-OMe

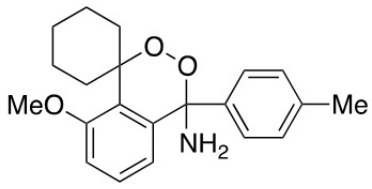

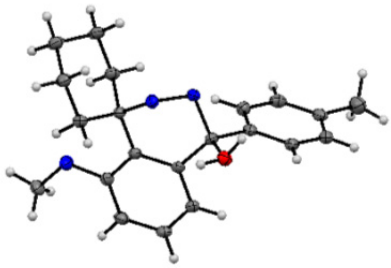

60% yield from 2-cyclohexyl-3-methoxybenzonitrile[6] and and *p*-tolylmagnesium bromide; Colorless Crystals (CCDC 891345); mp. 201.7-221.7 °C; IR (ATR) 3588 3566 1522 1506 1472 1246 cm^{-1}; ^1H NMR (400 MHz, $CDCl_3$) δ 1.47 – 1.30 (1H, m), 1.97 – 1.48 (7H, m), 2.18 (1H, br), 2.32 (3H, s), 2.44 (1H, br), 2.79 (2H, br), 3.85 (3H, s), 6.59 (1H, br), 6.76 (1H, br), 7.05 (1H, br), 7.12 (2H, d, J = 7.9 Hz), 7.39 (2H, d, J = 7.9 Hz); ^{13}C NMR (100 MHz, $CDCl_3$) δ 21.4, 21.8, 21.9, 25.5, 31.2, 31.4, 55.5, 81.6, 92.2, 110.1, 121.5, 127.2, 127.3, 129.0 (overlapped), 129.5, 138.3, 140.4, 155.6; EIHRMS: Found: *m/z* 340.1928. Calcd for $C_{21}H_{26}NO_3$: $(M+H)^+$ 340.1913.

Procedure for Functionalization of Amino Endoperoxide 1: Synthesis of Azido Endoperoxide, (13) N_3

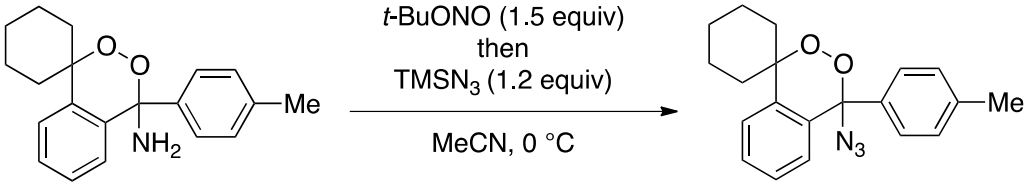

1 **13** 60%

To a solution of 4-(*p*-tolyl)-4*H*-spiro[benzo[*d*][1,2]dioxine-1,1'-cyclohexan]-4-amine, **1** (115 mg, 0.370 mmol) in anhydrous MeCN (3.0 mL) under N_2 atmosphere at 0 °C was added 90% *tert*-Butyl nitrite (74 µL, 0.600 mmol, 1.5 equiv). The mixture was stirred at 0 °C under N_2 atmosphere for 5 min, azidotrimethylsilane (59 µL, 0.445 mmol, 1.2 equiv) was added. The mixture was allowed to stirred at rt for 17 h. Upon completion of the reaction, solvents were removed under reduced pressure, the resulting crude materials were purified by flash column chromatography (Hexane : ethyl acetate = 9 : 1) to afford 4-azido-4-(*p*-tolyl)-4*H*-spiro[benzo[*d*][1,2]dioxine-1,1'-cyclohexane] (**13**) (74.5 mg ,0.222 mmol) in 60 % yield. The solid was recrystallized from hexane/ethyl acetate for biological assay.

4-azido-4-(*p*-tolyl)-4*H*-spiro[benzo[*d*]|[1,2]dioxine-1,1'-cyclohexane], (13) N_3

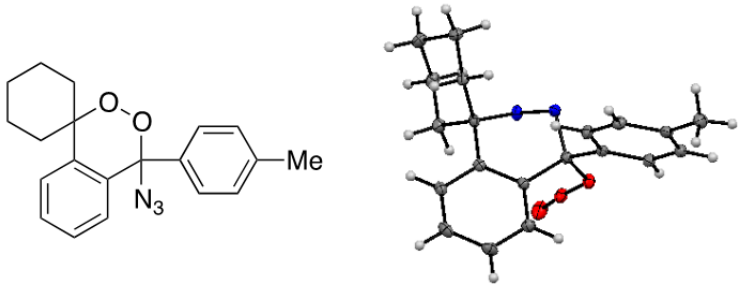

Colorless Crystals (CCDC 891347); mp. 165.9-167.2 °C (exclusion of gas); IR (ATR) 2124 1242, 1522, 1506, 1449, 1242 cm^{-1}; ^1H NMR (400 MHz, $CDCl_3$) δ 1.47 – 1.28 (1H, m), 1.92 – 1.53 (7H, m), 2.12 (1H, ddd, J = 18.3, 12.1, 4.2 Hz), 2.32 (3H, s), 2.59 – 2.43 (1H, m), 6.94 (1H, d, J = 7.2 Hz), 7.16 – 7.07 (2H, m), 7.26 – 7.16 (1H, m), 7.40 – 7.26 (4H, m); ^{13}C NMR (100 MHz, $CDCl_3$) δ 21.4, 21.5, 21.9, 25.5, 34.9, 35.3, 81.8, 98.5, 123.8, 127.2, 128.0, 128.0, 129.0, 129.1, 132.4, 134.3, 139.9, 141.7; EIHRMS: Found: *m/z* 336.1699. Calcd for $C_{20}H_{22}N_3O_2$: $(M+H)^+$ 336.1712.

Procedure for Functionalization of Amino Endoperoxide 1: Synthesis of Hydroxy Endoperoxide, (14) OH

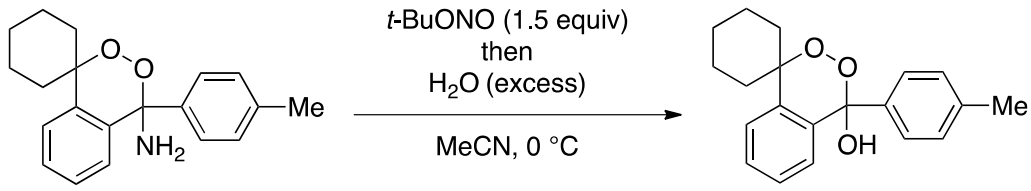

1 **14** 79%

To a solution of 4-(*p*-tolyl)-4*H*-spiro[benzo[*d*][1,2]dioxine-1,1'-cyclohexan]-4-amine **1** (62.2 mg, 0.201 mmol) in anhydrous MeCN (2.0 mL) under N_2 atmosphere at 0 °C was added 90% *tert*-Butyl nitrite (36 µL, 0.272 mmol, 1.5 equiv). The mixture was stirred at 0°C under N_2 atmosphere for 5 mins, water (1 mL, 55.6 mmol, 276 equiv) was added. The mixture was allowed to stirr at rt for 24 h. Upon completion of the reaction, solvents were removed under reduced pressure, the resulting crude materials were purified by flash column chromatography (hexane : ethyl acetate = 9 : 1) to afford 4-(*p*-tolyl)-4*H*-spiro[benzo[*d*][1,2]dioxine-1,1'-cyclohexan]-4-ol **(14)** (49.3 mg, 0.159 mmol) in 79% yield. The solid was recrystallized from hexane/ethyl acetate for biological assay.

4-(*p*-tolyl)-4*H*-spiro[benzo[*d*][1,2]dioxine-1,1'-cyclohexan]-4-ol, (14) OH

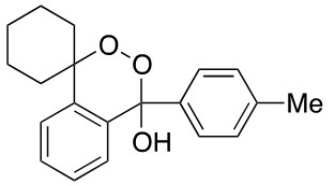

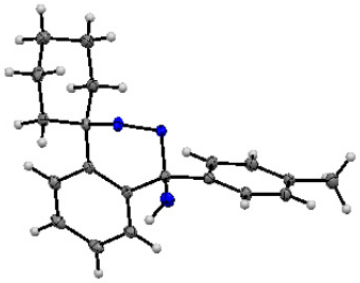

Pale Yellow Crystals (CCDC 891349); mp. 134.9-135.9 °C; IR (ATR) 3437, 2936, 1508, 1447 m^{-1}; ^1H NMR (400 MHz, $CDCl_3$) δ 1.49 – 1.16 (2H, m), 1.98 – 1.52 (6H, m), 2.09 (1H, td, *J* = 13.8, 4.7 Hz), 2.35 (3H, s), 2.62 – 2.47 (1H, m), 4.06 (1H, s), 7.06 – 6.95 (1H, m), 7.19 – 7.08 (3H, m), 7.26 – 7.19 (1H, m), 7.35 – 7.26 (1H, m), 7.46 – 7.35 (2H, m); ^{13}C NMR (100 MHz, $CDCl_3$) δ 21.2, 21.3, 21.8, 25.4, 34.4, 35.0, 81.3, 100.8, 123.3, 126.7, 127.4, 128.2, 128.3, 128.7, 135.7, 136.1, 139.0, 140.9; EIHRMS: Found: *m/z* 311.1638. Calcd for $C_{20}H_{23}O_3$: $(M+H)^+$ 311.1647.

Procedure for Synthesis of Amino Endoperoxide (15) Bearing An Alkynyl Moiety

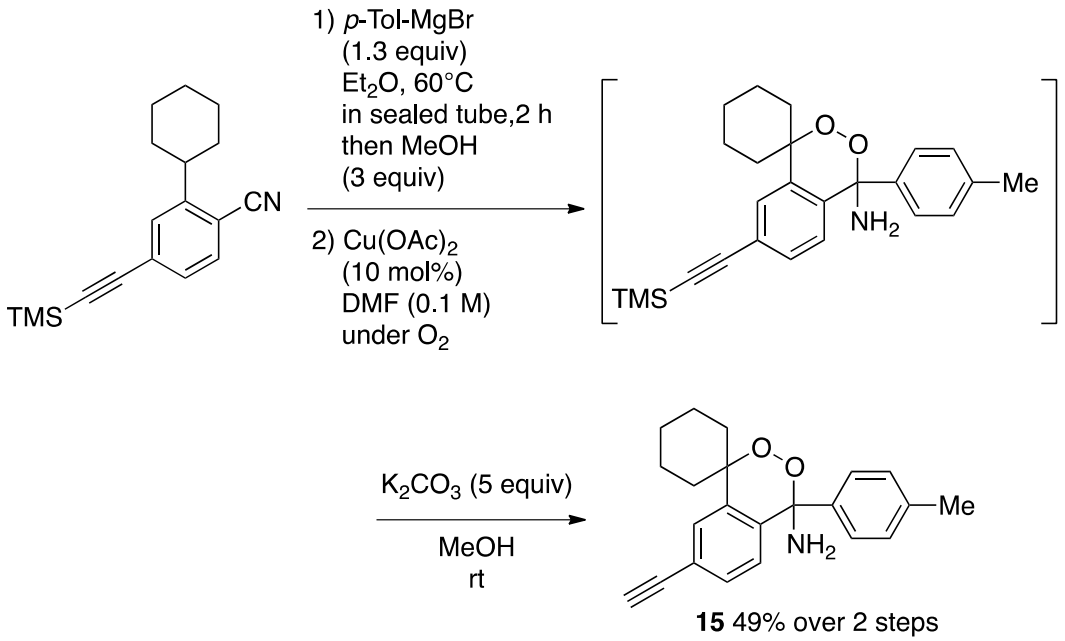

To a solution of 2-cyclohexyl-4-((trimethylsilyl)ethynyl)benzonitrile (109 mg, 0.387 mmol) in Et_2O (0.5 mL) was added an Et_2O solution of *p*-tolylmagnesium bromide (1.3 equiv). The reaction mixture was stirred at 60 °C in a sealed tube for 2 h. Anhydrous MeOH (39 μL, 3 equiv) was then added. $Cu(OAc)_2$ (7.7 mg, 10 mol%) and anhydrous DMF (5 ml) was then added. The reaction mixture was stirred at 80 °C under an oxygen atmosphere for 3 h. The reaction was quenched with pH 9 buffer solution and extracted three times with Et_2O (20 mL). The combined organic extracts were washed with water and brine. After drying with $MgSO_4$, the solvents were removed under reduced pressure. The resulting crude material were purified by flash column chromatography (Hex : EA = 95 : 5) to afford 4-(*p*-tolyl)-7-((trimethylsilyl)ethynyl)-4*H*-spiro[benzo[*d*][1,2]dioxine-1,1'-cyclohexan]-4-amine (115 mg, 0.283 mmol) in 73% yield, which was further used for the next TMS-deprotection step.

To a solution of the endoperoxide (115 mg, 0.283 mmol) in anhydrous MeOH (2.8 mL) was added potassium carbonate (196 mg, 1.42 mmol, 5 equiv). The reaction mixture was stirred at rt in under N_2 atmosphere for 2 h. Upon completion of the reaction, the mixture was filtered through a Celite pad washing with MeOH. After removal of solvents under reduced pressure, the resulting crude materials were purified by flash column chromatography (hexane : ethyl acetate = 9 : 1) to afford 7-ethynyl-4-(*p*-tolyl)-4*H*-spiro[benzo[*d*][1,2]dioxine-1,1'-cyclohexan]-4-amine (**15**) (63.6 mg, 0.189 mmol) in 67 % yield (49% over 2 steps). The solid was recrystallized from hexane/ethyl acetate for biological assay.

7-ethynyl-4-(*p*-tolyl)-4*H*-spiro[benzo[*d*][1,2]dioxine-1,1'-cyclohexan]-4-amine, (15)

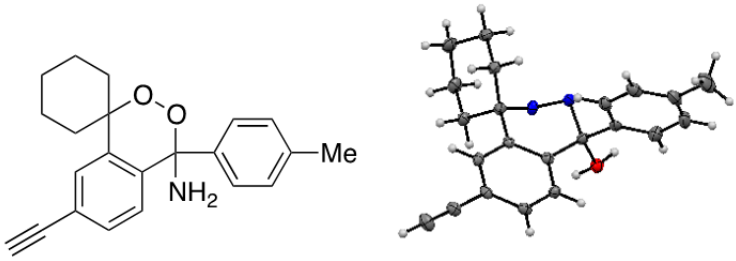

Colorless Crystals (CCDC 891351); mp. 189.9-190.6 °C; IR (ATR) 3566 3524 3482 3298 2311 1219 cm^{-1}; ^1H NMR (400 MHz, $CDCl_3$) δ 1.41 – 1.21 (2H, m), 2.02 – 1.52 (9H, m), 2.30 (3H, s), 2.44 (1H, br), 2.71 (2H, br), 3.05 (1H, s), 7.03 (1H, br), 7.18 – 7.09 (2H, m), 7.27 – 7.18 (1H, m), 7.43 – 7.30 (3H, m); ^{13}C NMR (100 MHz, $CDCl_3$) δ 21.3, 21.7, 21.9, 25.6, 35.2, 35.5, 81.2, 83.5, 92.3, 121.3, 127.1, 127.8, 128.7, 129.2 (overlapped), 130.2, 138.4, 138.7, 141.4; EIHRMS: Found: *m/z* 334.1816. Calcd for $C_{22}H_{24}NO_2$: $(M+H)^+$ 334.1807.

2-cyclohexyl-4-((trimethylsilyl)ethynyl)benzonitrile (the preparation scheme was shown below)

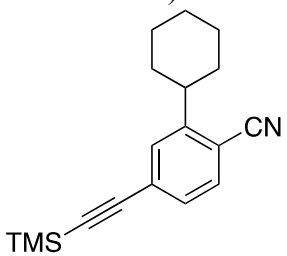

Brown solid; mp. 68.2-70.6 °C; IR (ATR) 3647, 2156, 1522, 1506 cm^{-1}; ^1H NMR (400 MHz, $CDCl_3$) δ 0.23 (9H, s), 1.27 (1H, dd, J = 12.6, 9.4 Hz), 1.53 – 1.34 (4H, m), 1.99 – 1.71 (5H, m), 3.03 – 2.86 (1H, m), 7.33 (1H, d, J = 8.0 Hz), 7.44 (1H, s), 7.52 (1H, d, J = 8.0 Hz); ^{13}C NMR (100 MHz, $CDCl_3$) δ 0.0, 26.1, 26.7, 33.7, 42.8, 98.7, 103.8, 111.7, 118.1, 128.1, 129.8, 130.3, 132.9, 151.6; EIHRMS: Found: *m/z* 282.1684. Calcd for $C_{18}H_{24}NSi$: $(M+H)^+$ 282.1678.

A synthetic scheme of 4-alkynylbenzonitrile

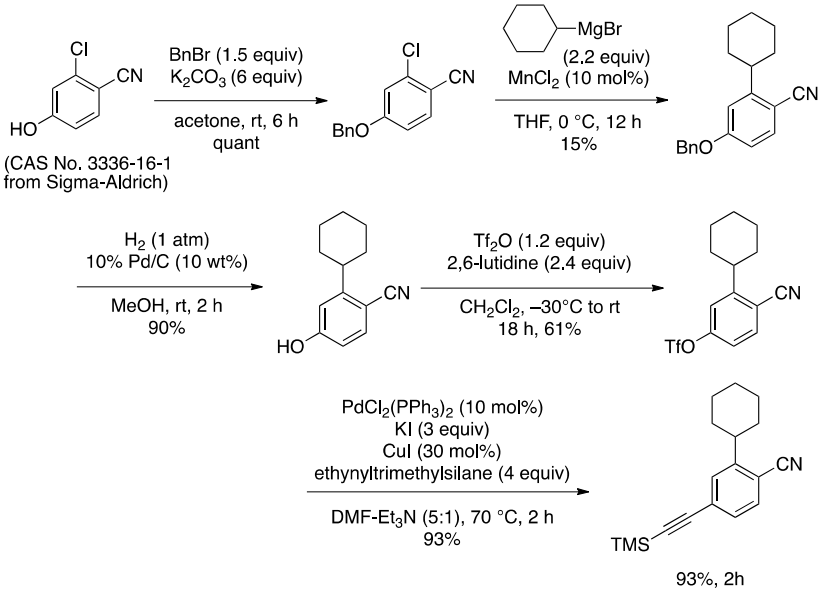

NMR Spectrum of New Compounds

^{1}H NMR of **(2)** (400 MHz, $CDCl_3$)

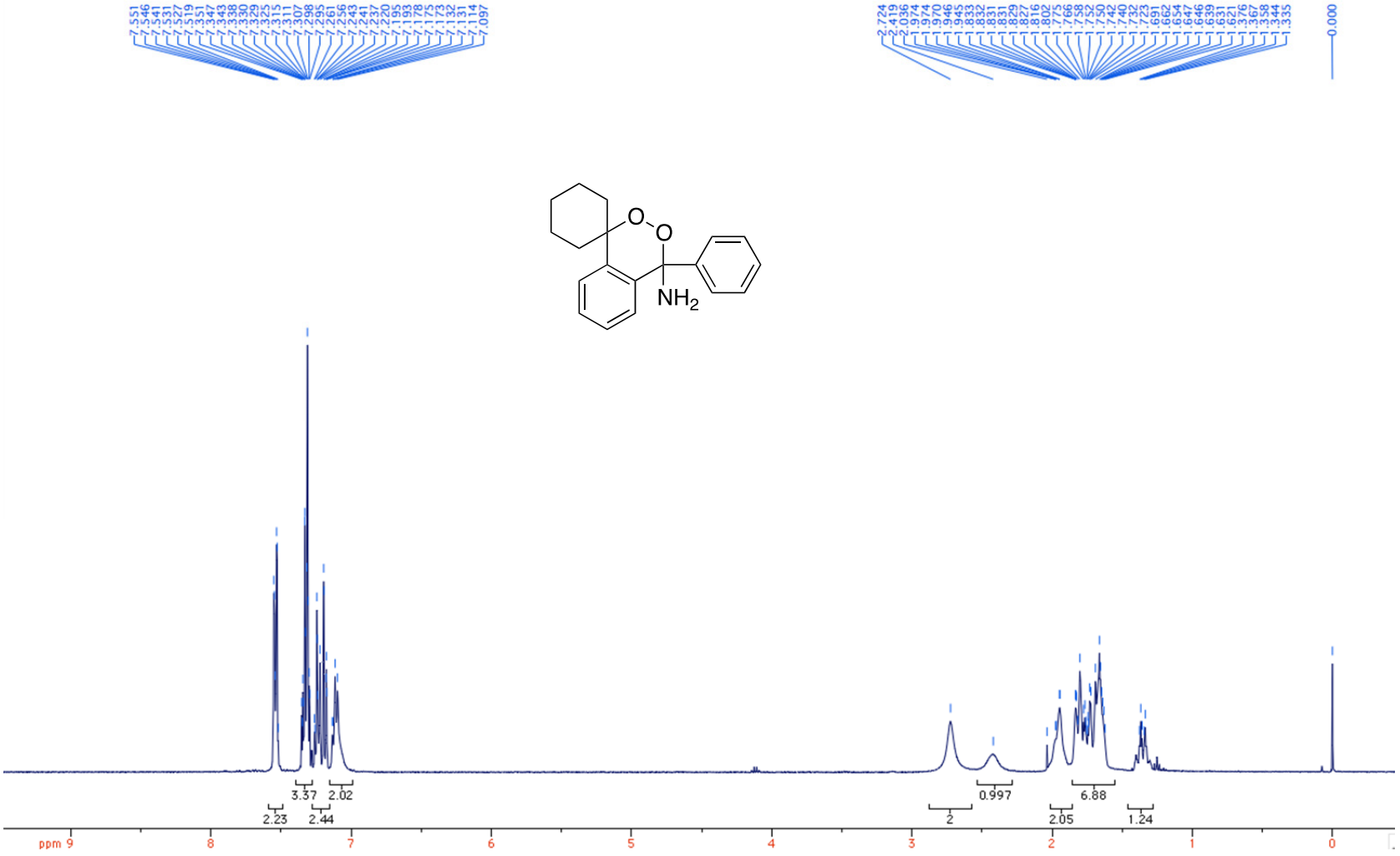

^{13}C NMR of **(2)** (100 MHz, $CDCl_3$)

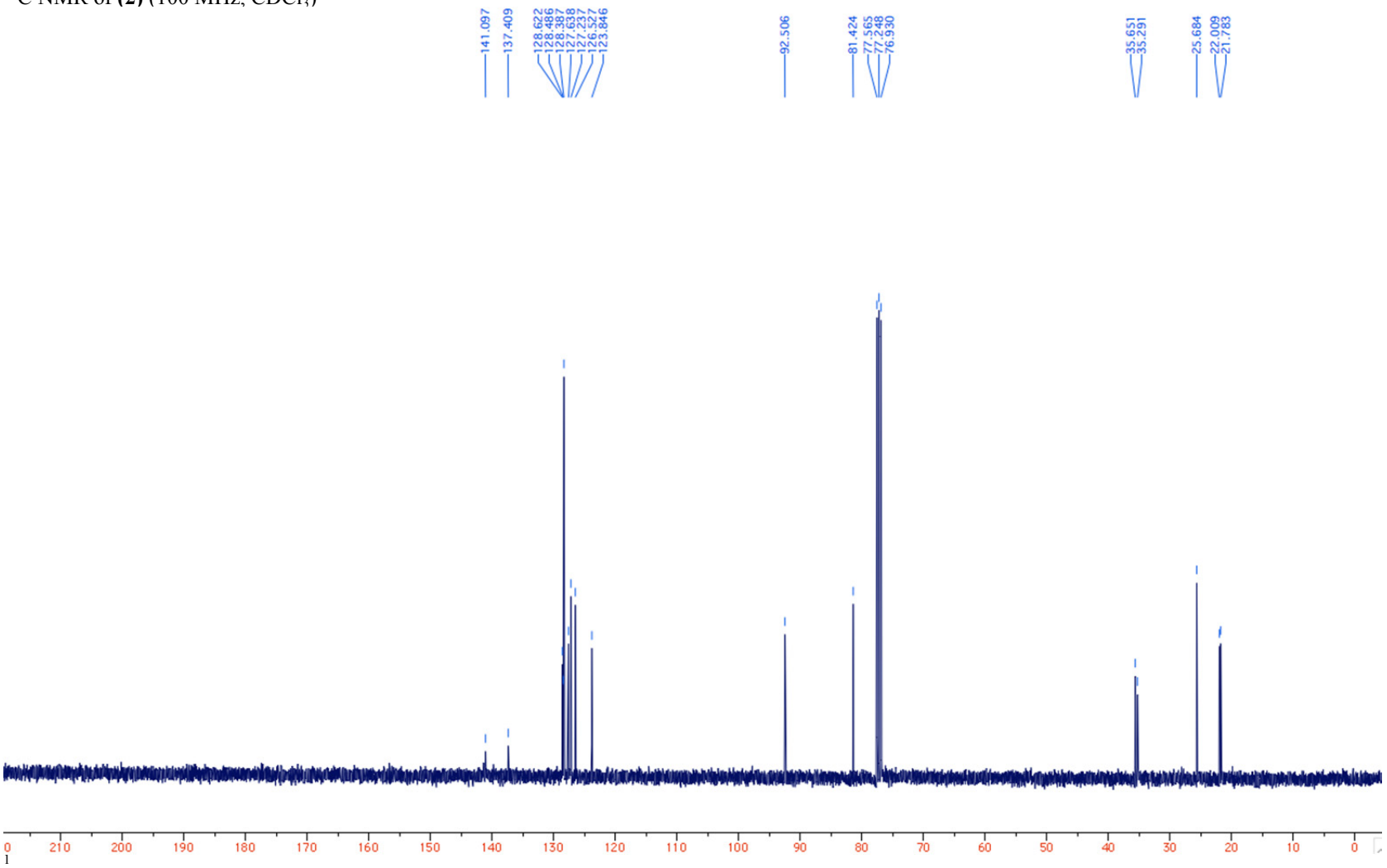

H NMR of **(3)** (400 MHz, $CDCl_3$)

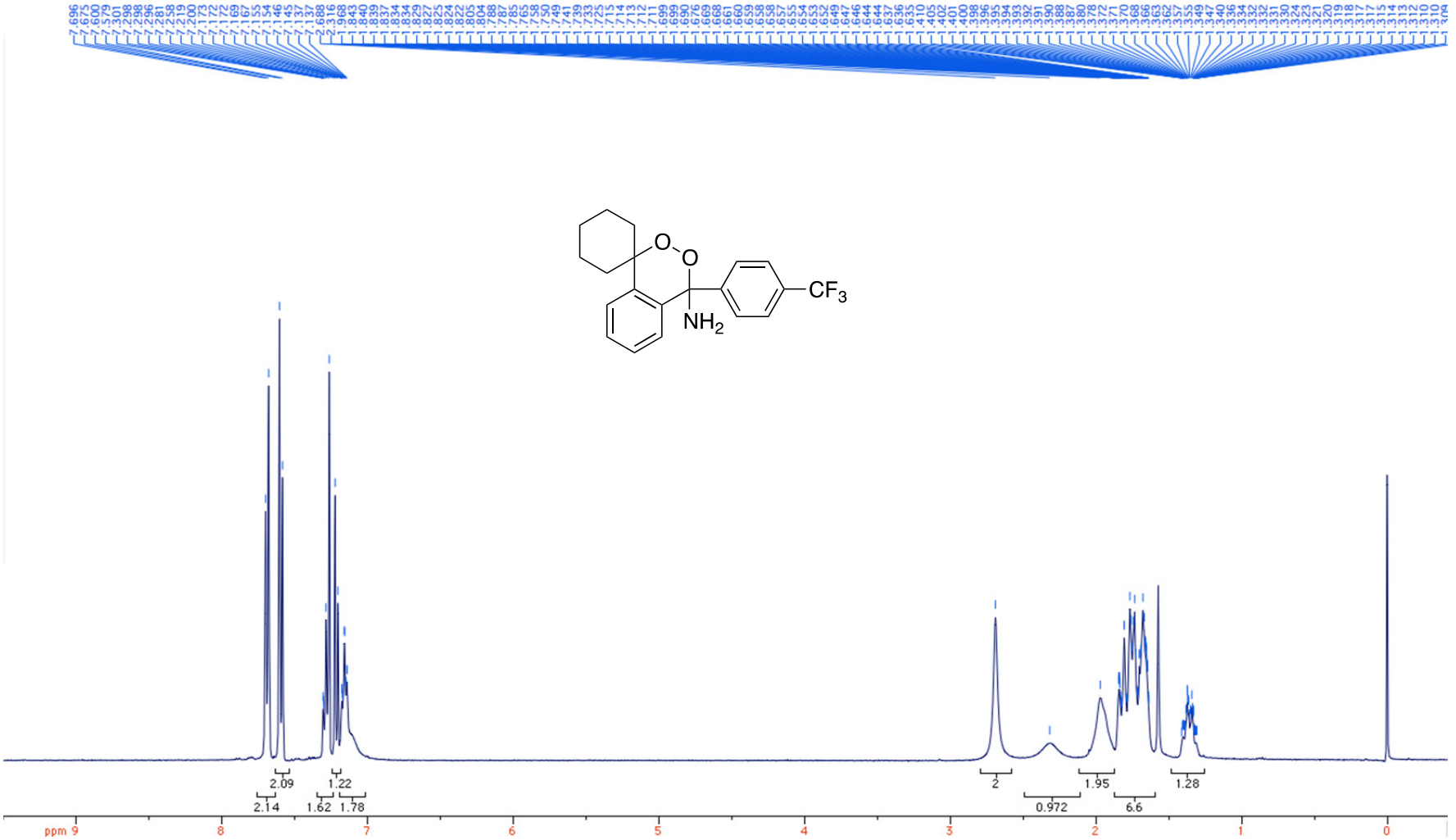

^{13}C NMR of **(3)** (100 MHz, $CDCl_3$)

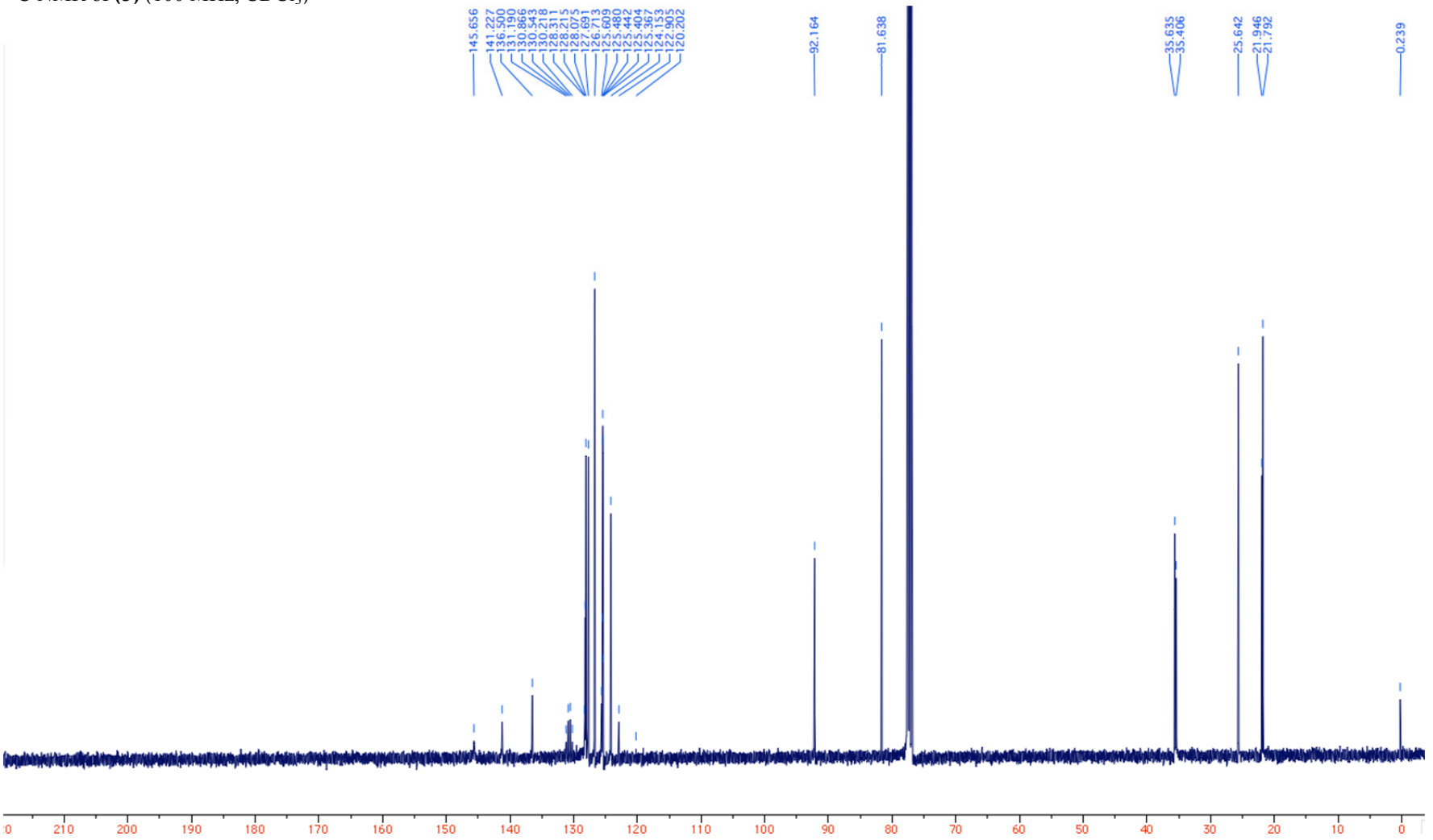

^{1}H NMR of **(4)** (400 MHz, $CDCl_3$)

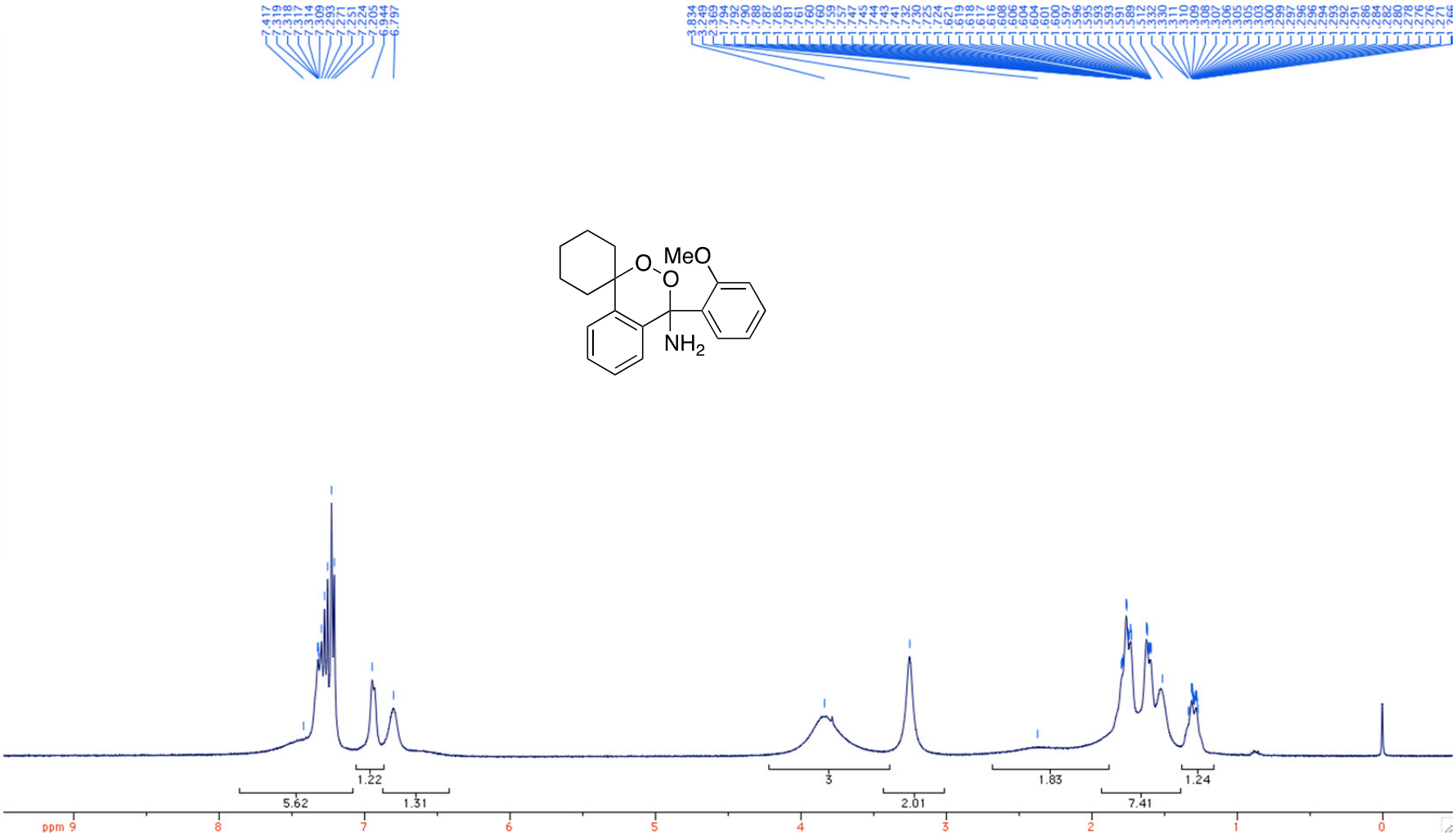

^{13}C NMR of **(4)** (100 MHz, $CDCl_3$)

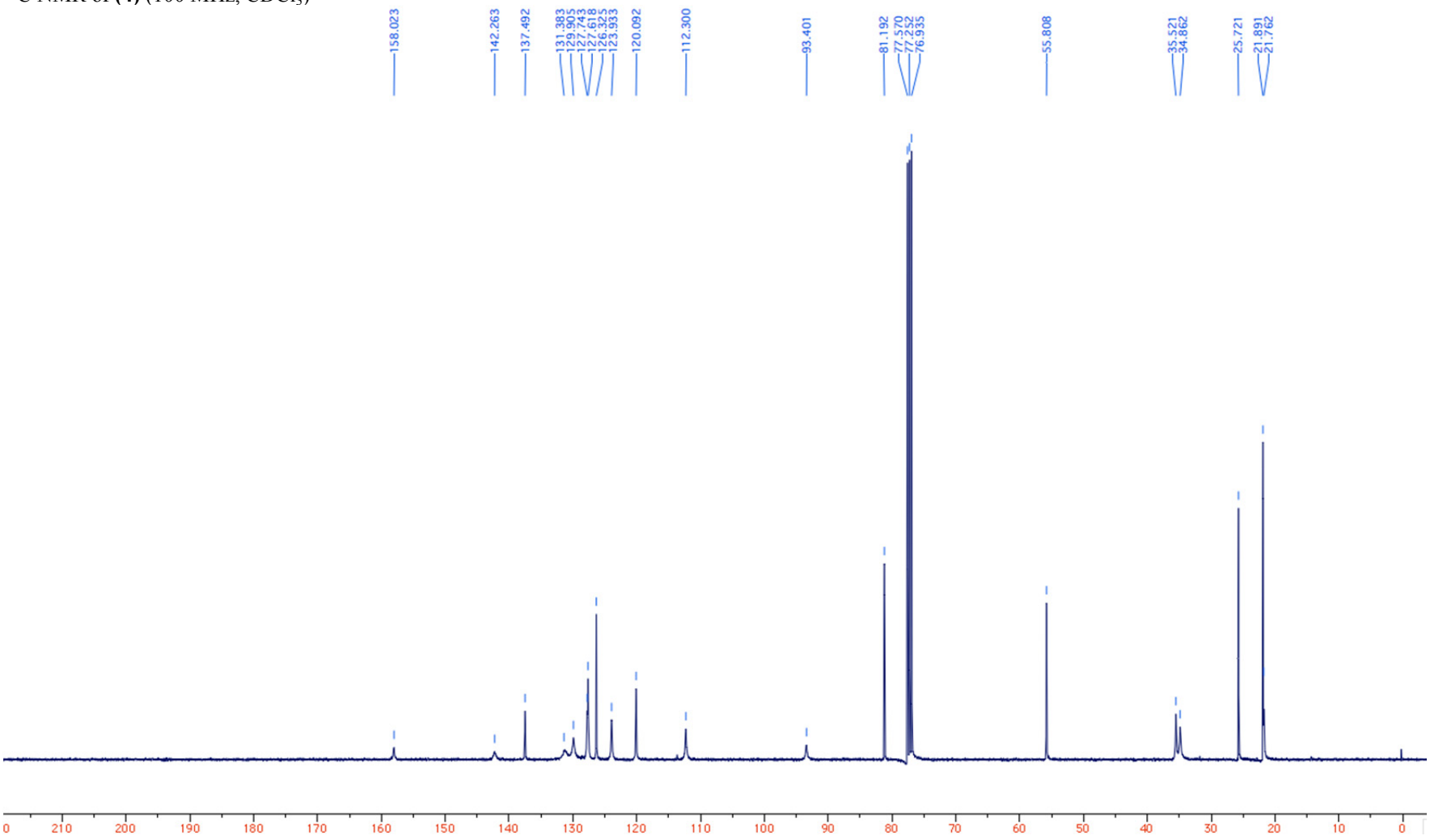

^{1}H NMR of **(5)** (400 MHz, $CDCl_3$)

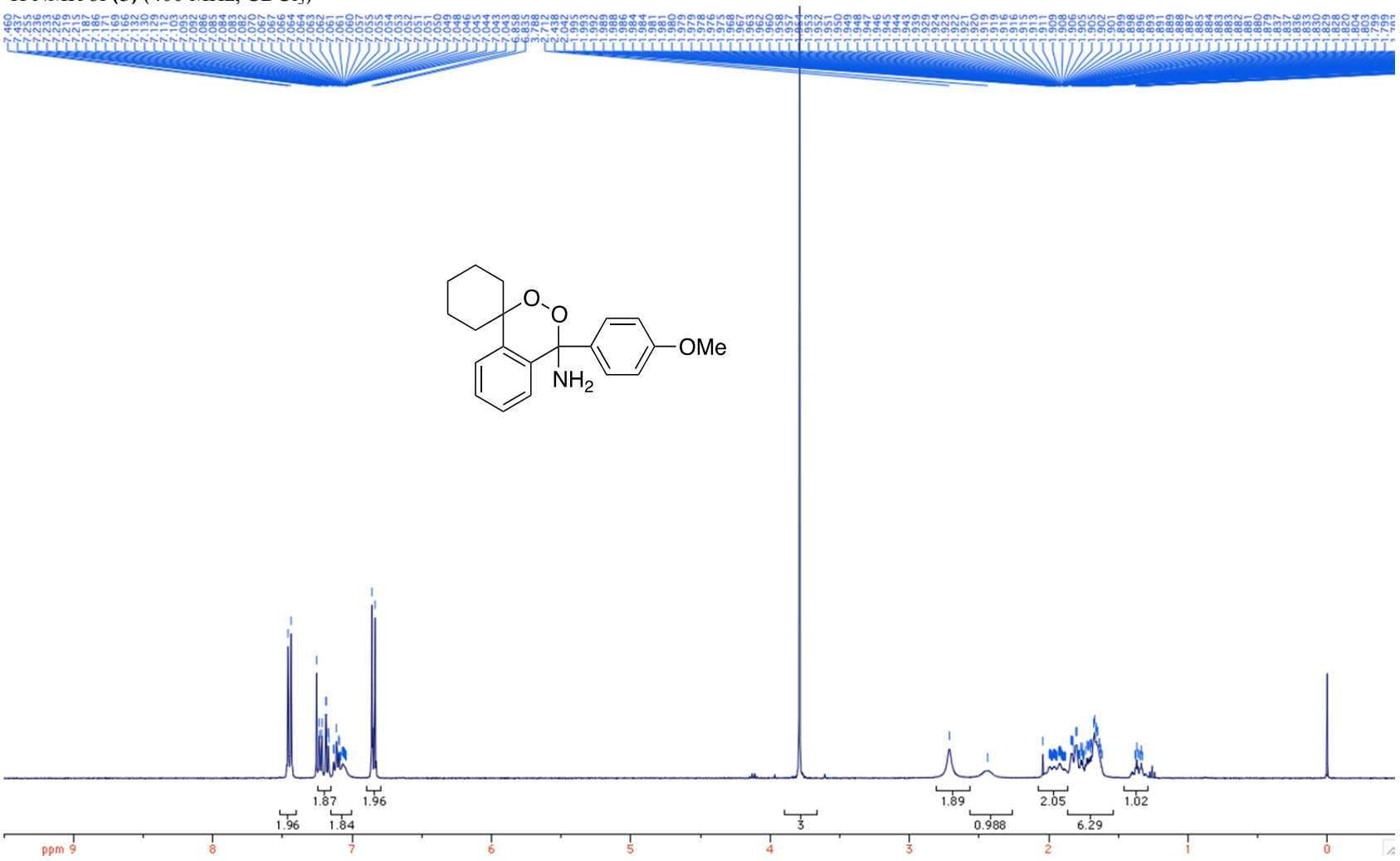

^{13}C NMR of **(5)** (100 MHz, $CDCl_3$)

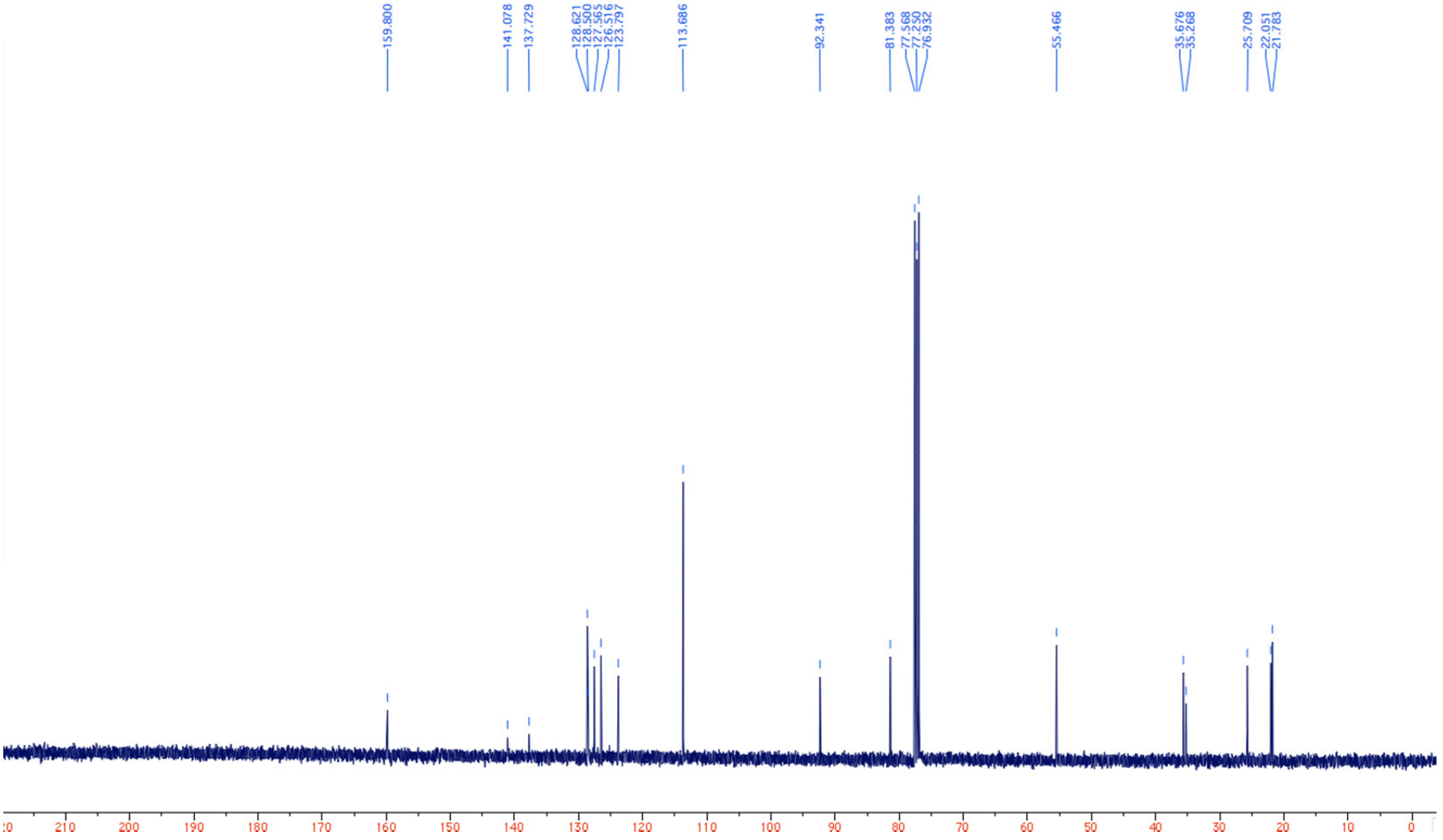

^{1}H NMR of **(6)** (500 MHz, $CDCl_3$)

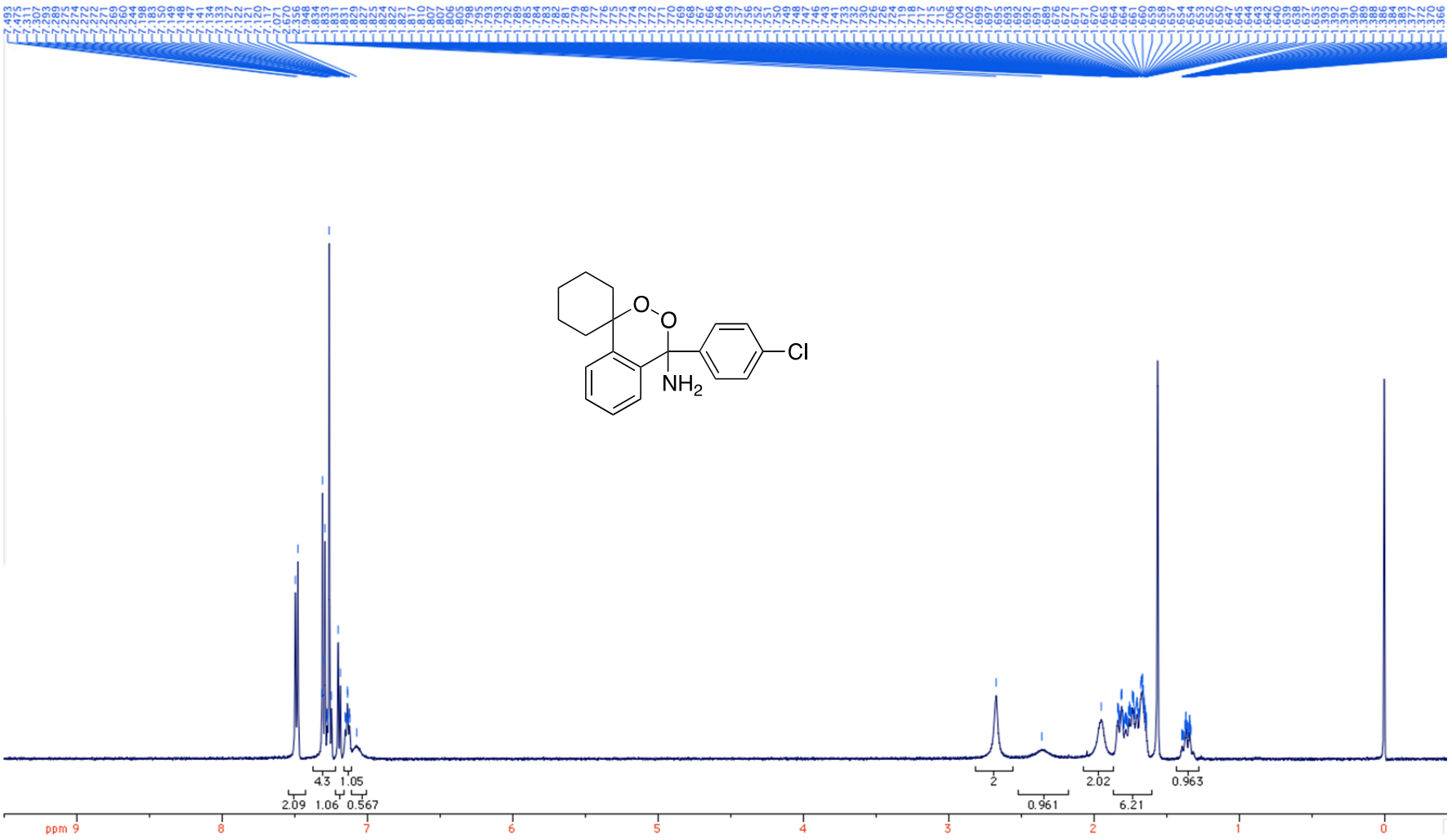

^{13}C NMR of **(6)** (100 MHz, $CDCl_3$)

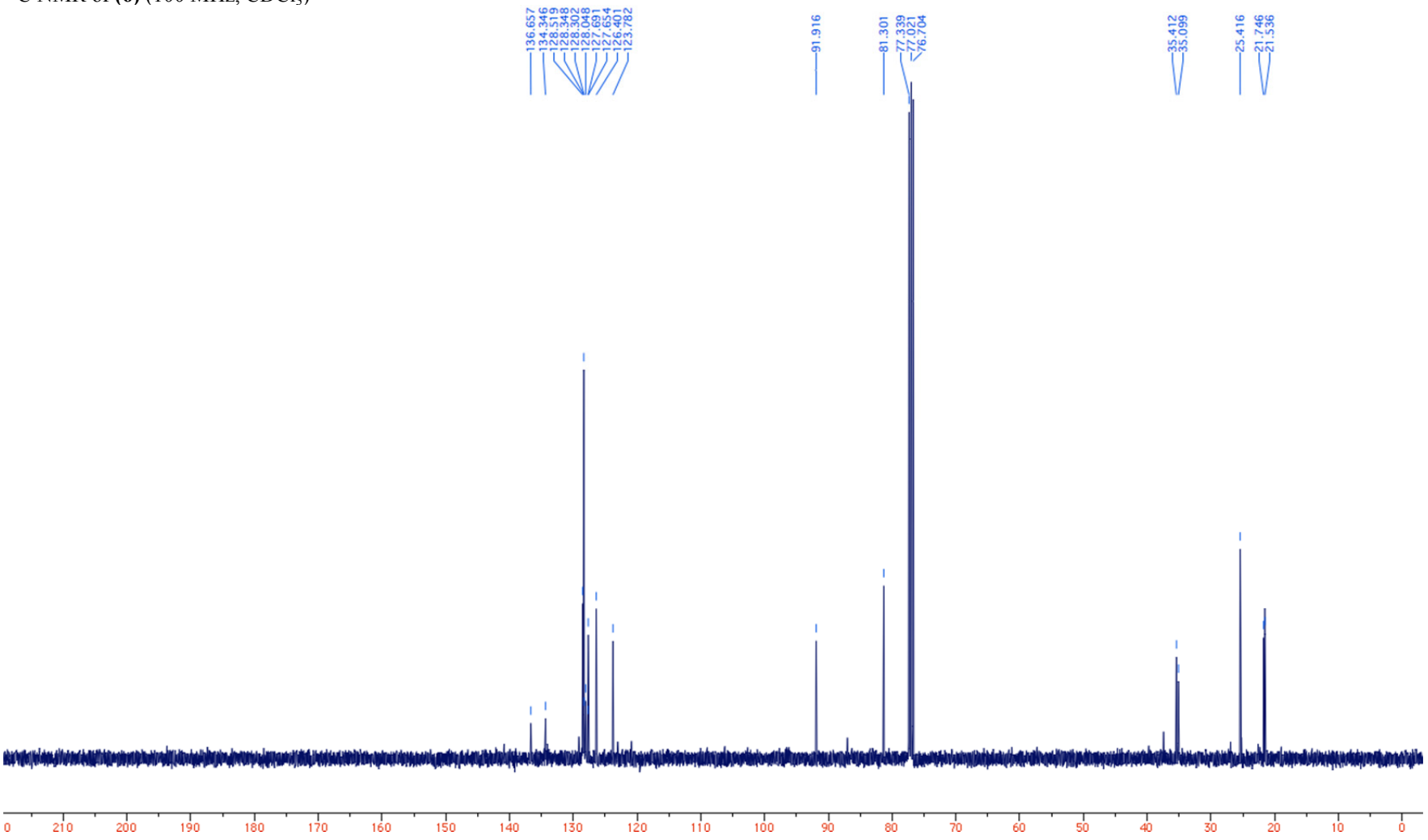

^{1}H NMR of **(7)** (400 MHz, $CDCl_3$)

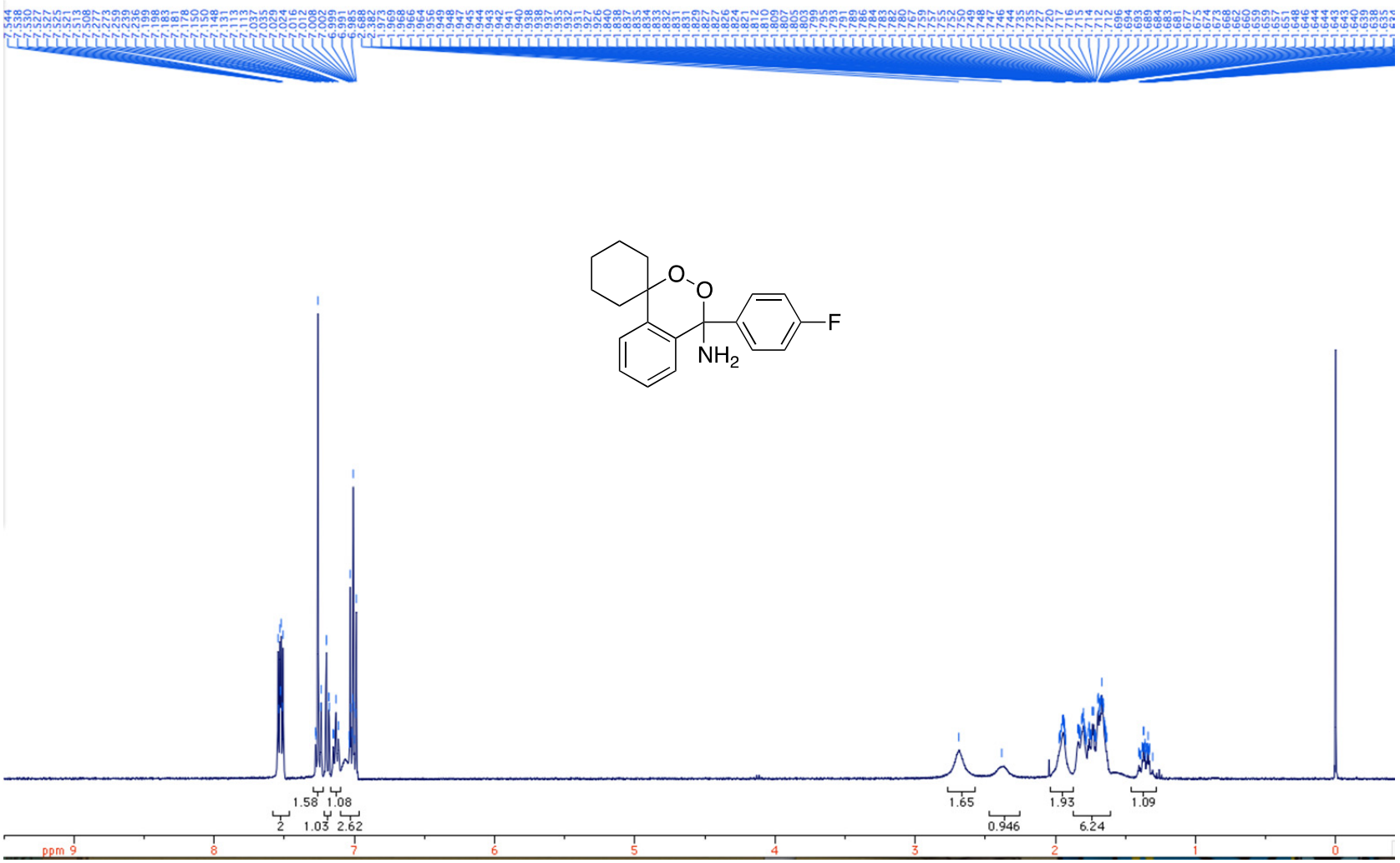

^{13}C NMR of **(7)** (100 MHz, $CDCl_3$)

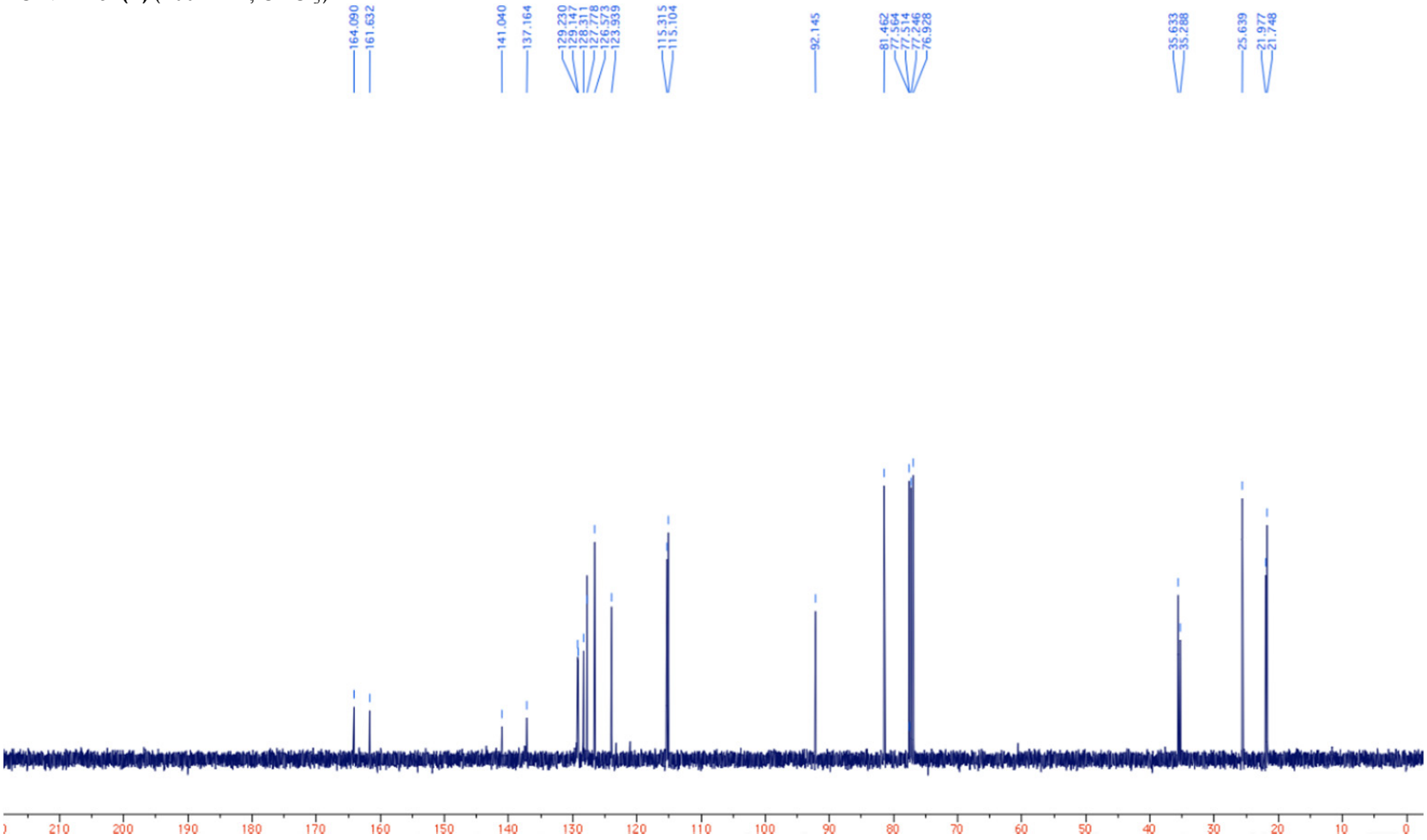

^{1}H NMR of **(8)** (400 MHz, $CDCl_3$)

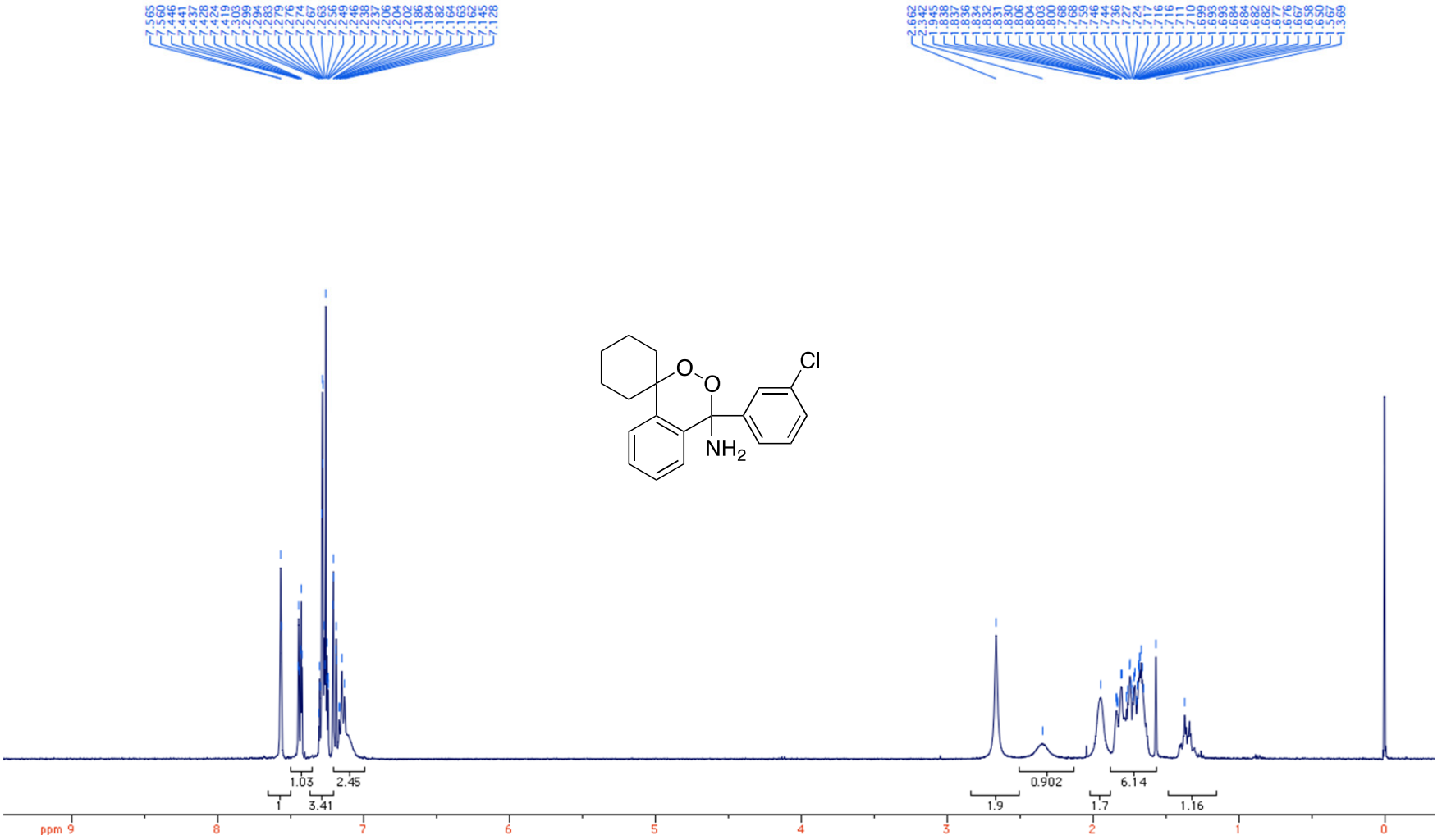

^{13}C NMR of **(8)** (100 MHz, $CDCl_3$)

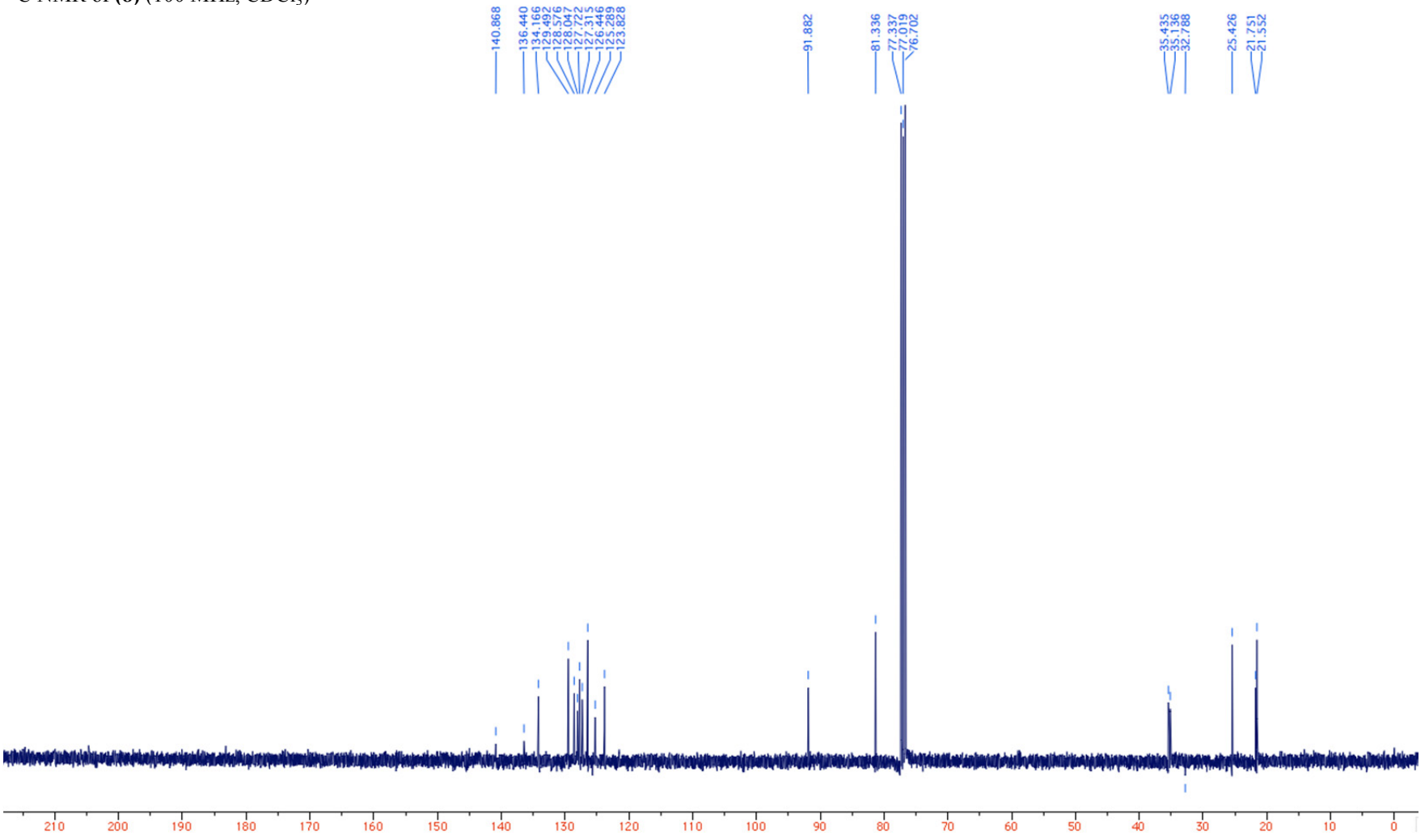

^{1}H NMR of **(9)** (400 MHz, $CDCl_3$)

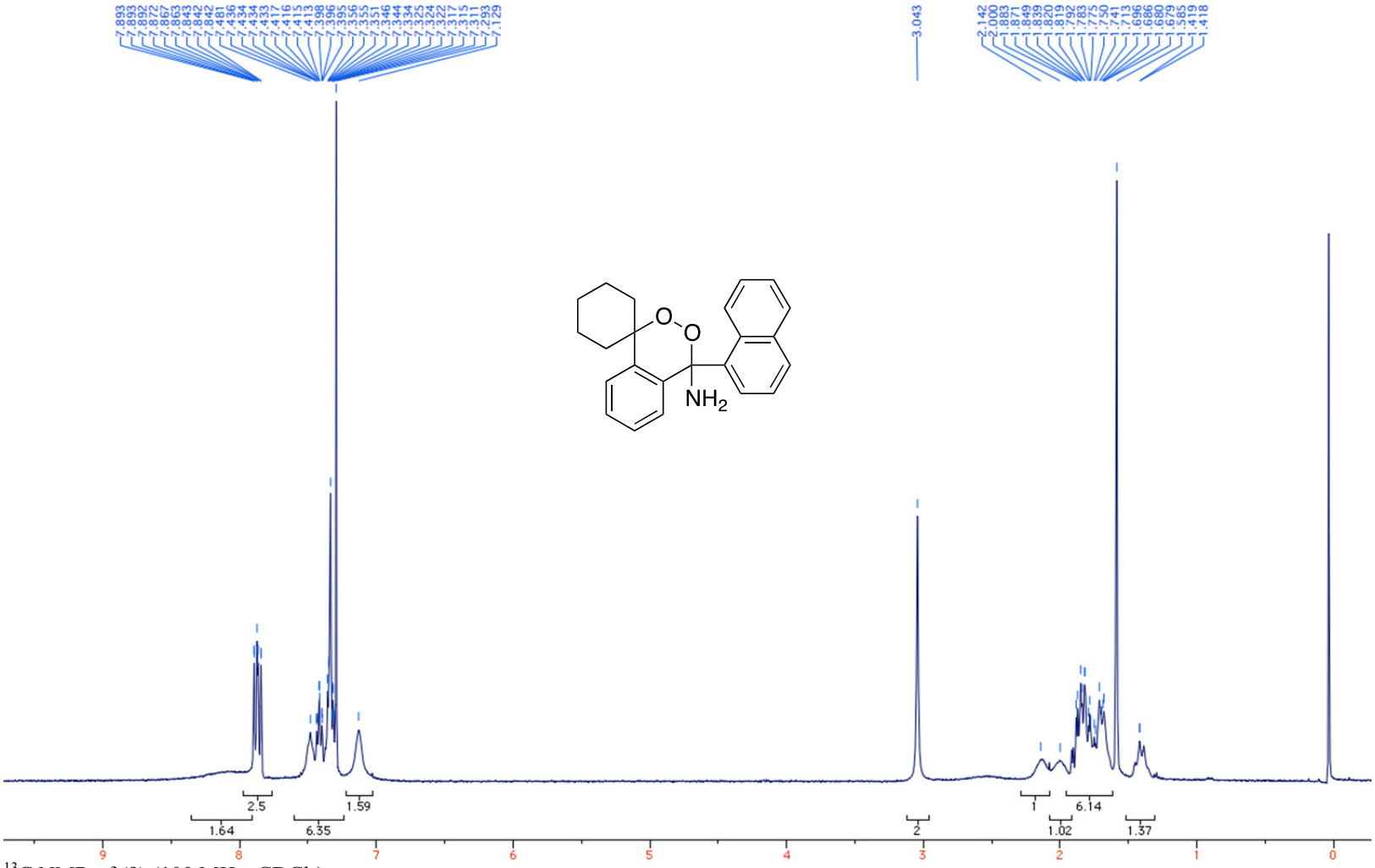

^{13}C NMR of **(9)** (100 MHz, $CDCl_3$)

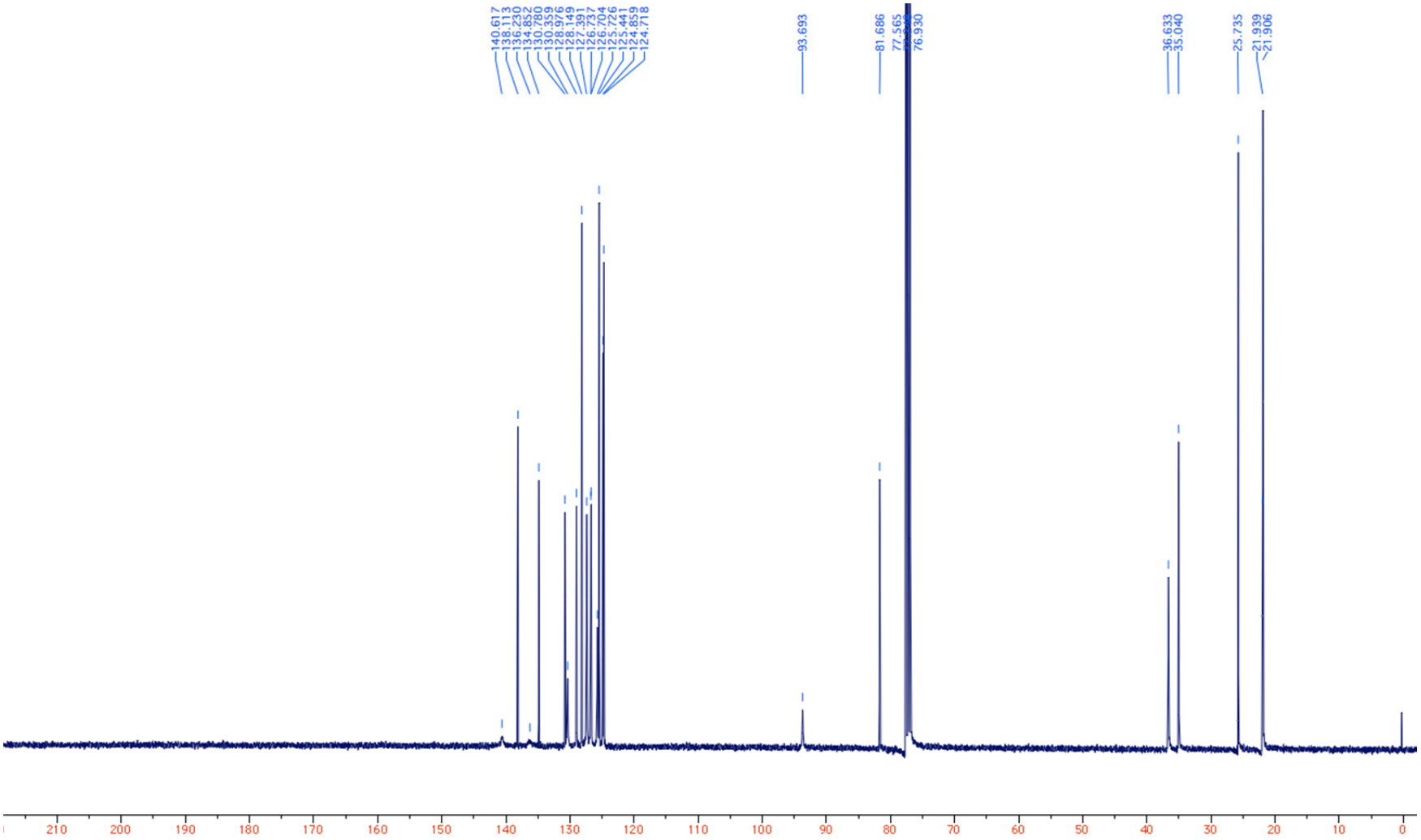
140.617
138.113
136.230
134.852
130.780
130.359
128.976
128.149
127.391
126.737
126.704
125.726
125.441
124.859
124.718
93.693
81.686
77.565
76.930
36.633
35.040
25.735
21.939
21.906
210
200
190
180
170
160
150
140
130
120
110
100
90
80
70
60
50
40
30
20
10
0

^{1}H NMR of **(10)** (400 MHz, $CDCl_3$)

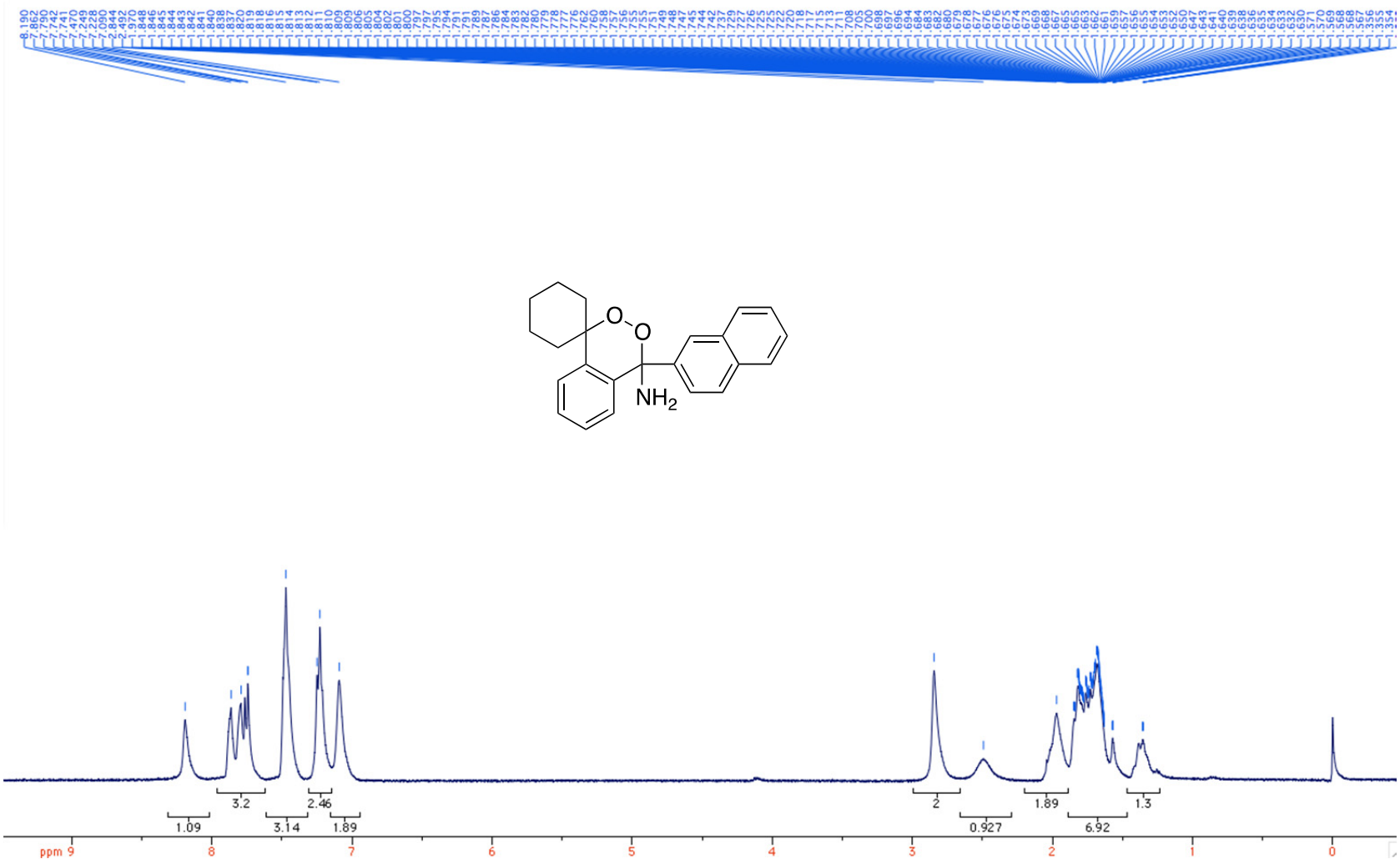

^{13}C NMR of **(10)** (100 MHz, $CDCl_3$)

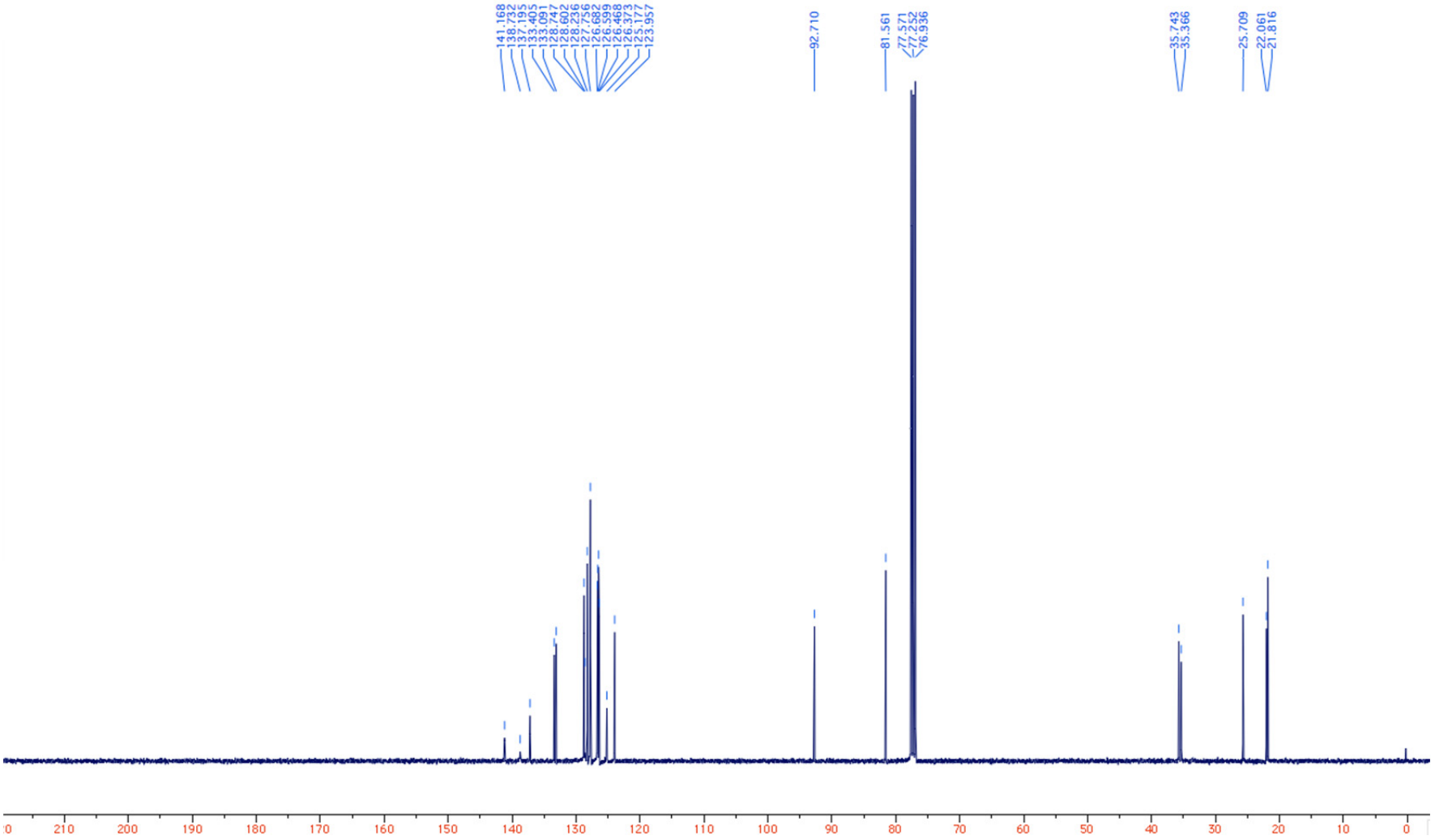

^{1}H NMR of **(11)** (400 MHz, $CDCl_3$)

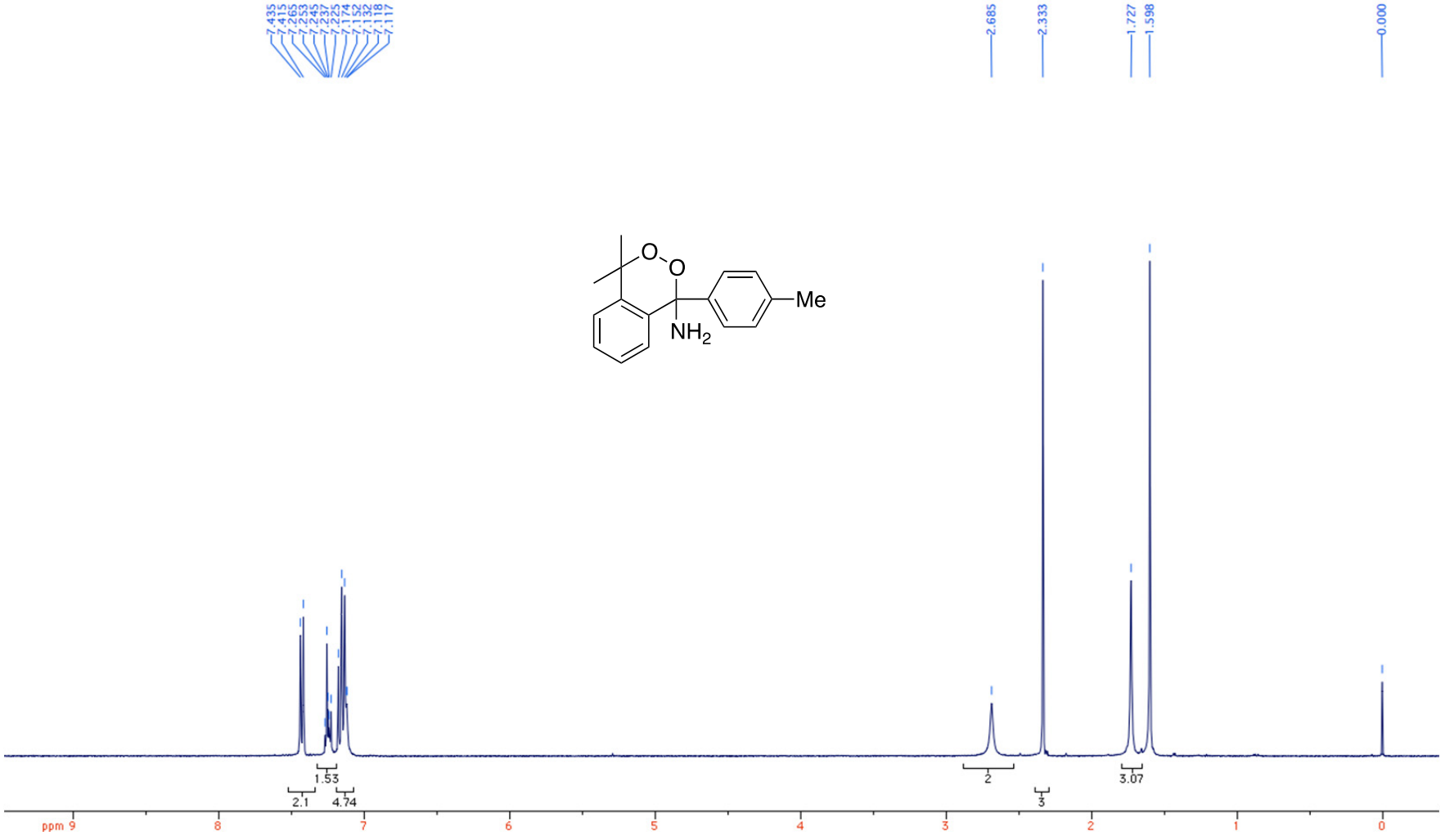

^{13}C NMR of **(11)** (100 MHz, $CDCl_3$)

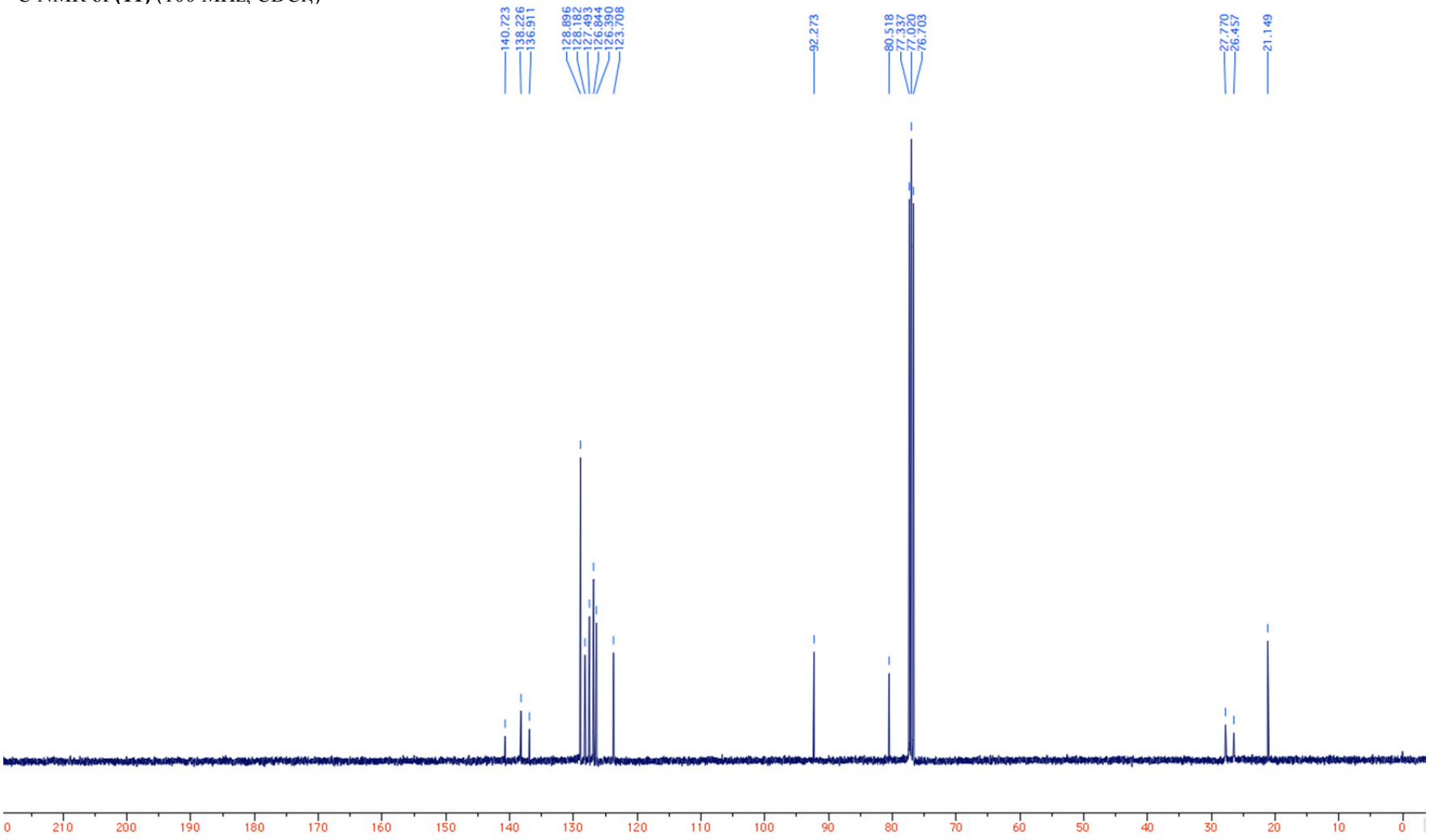

^{1}H NMR of **(12)** (400 MHz, $CDCl_3$)

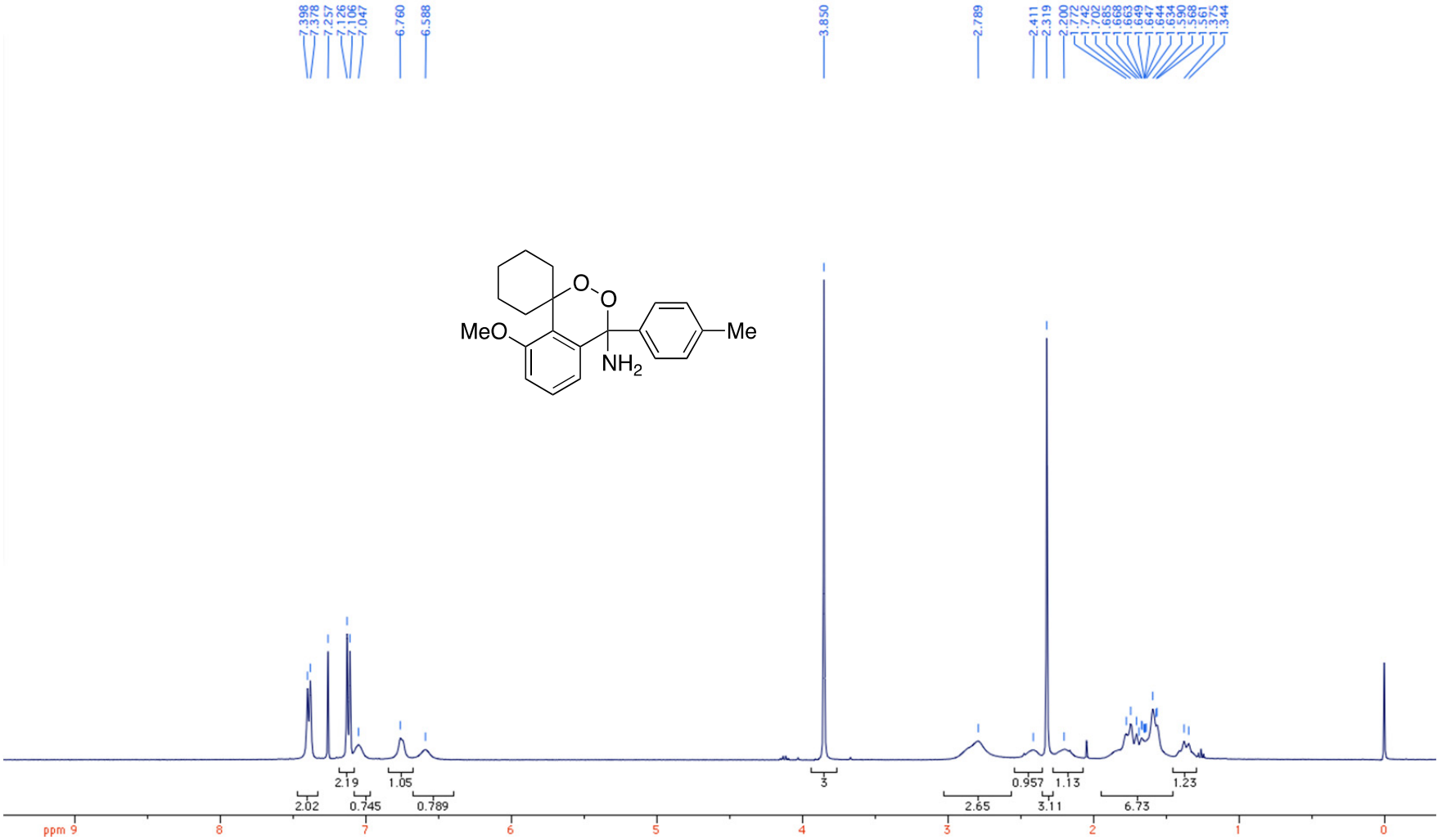

^{13}C NMR of **(12)** (100 MHz, $CDCl_3$)

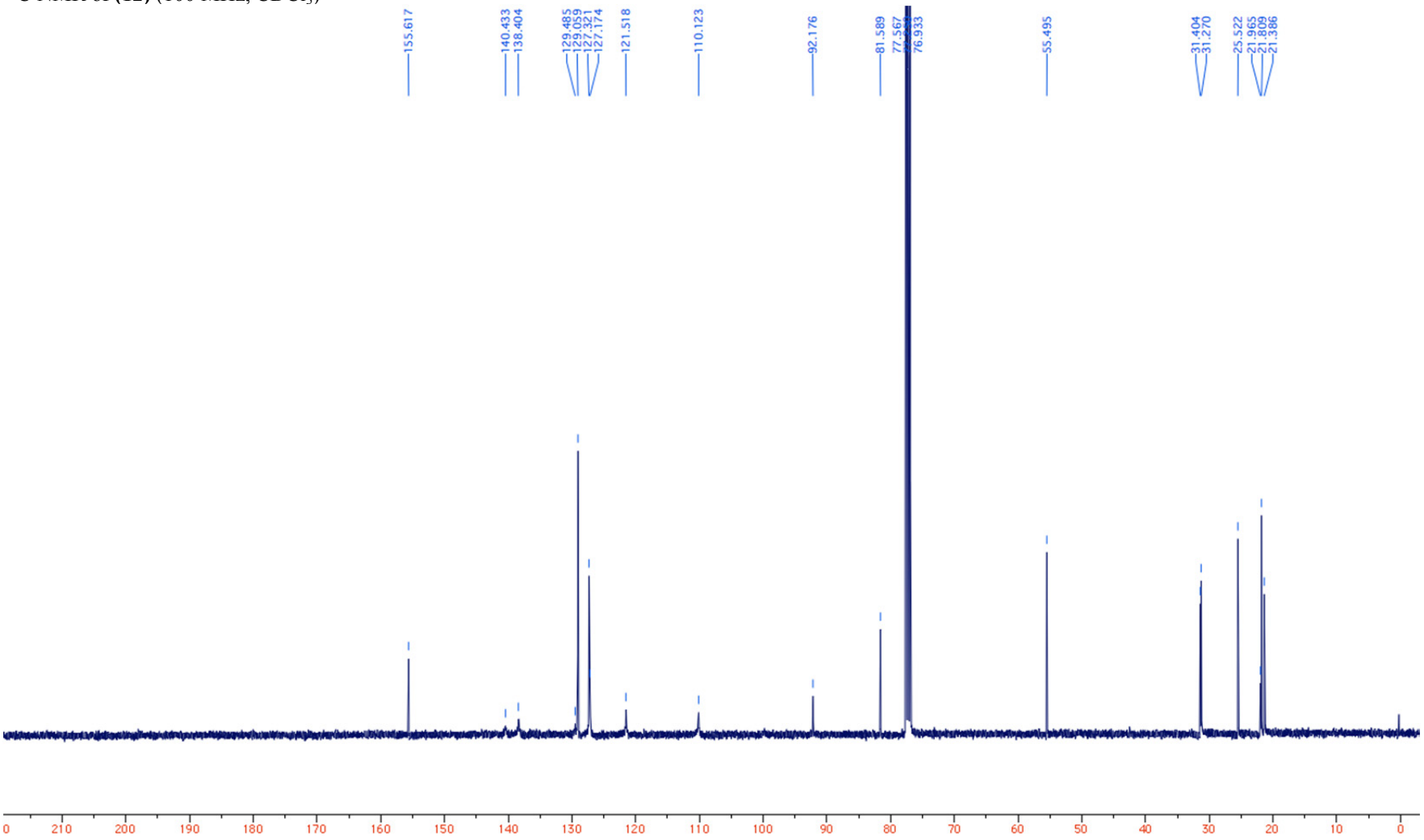

^{1}H NMR of **(13)** (400 MHz, $CDCl_3$)

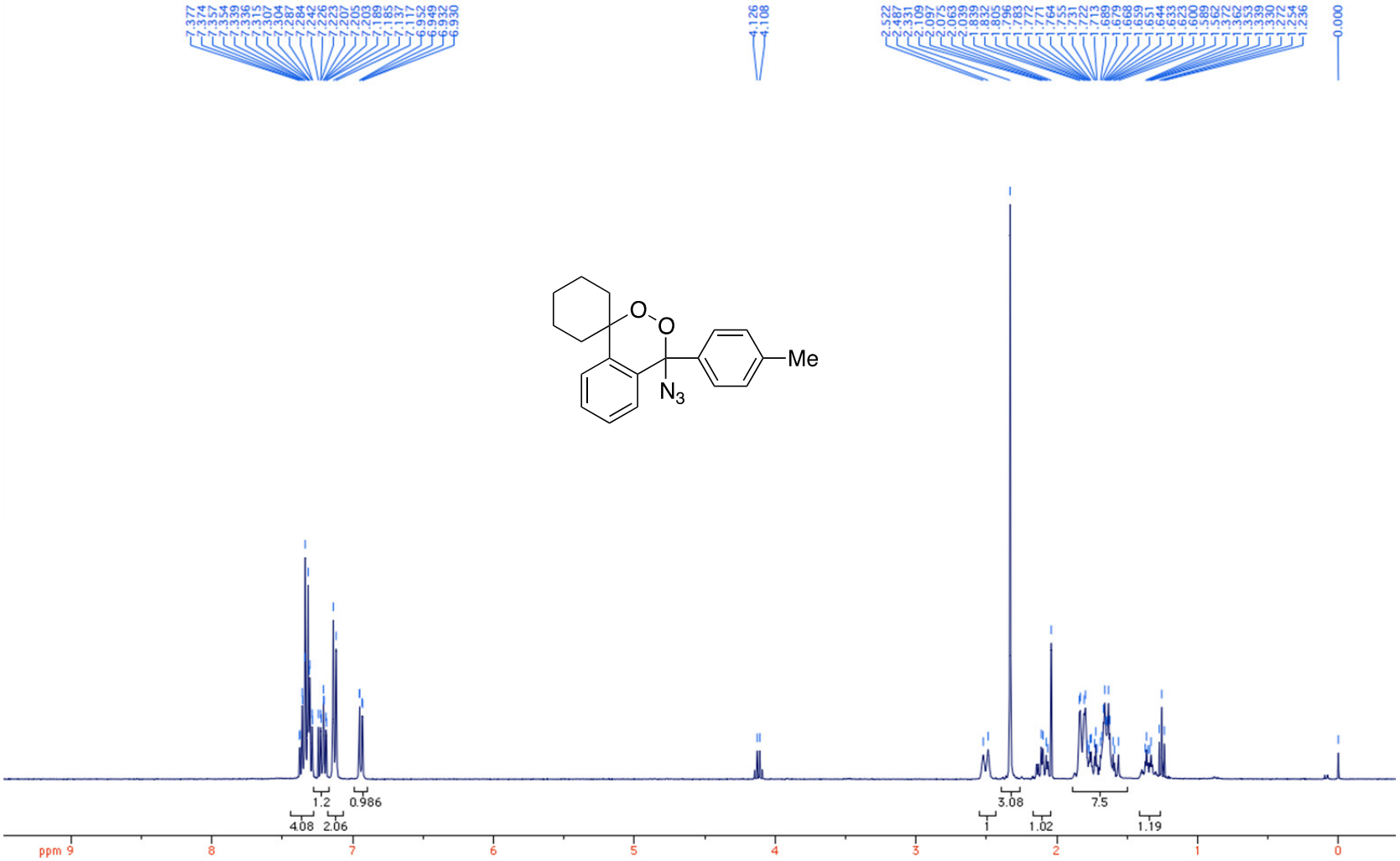

^{13}C NMR of **(13)** (100 MHz, $CDCl_3$)

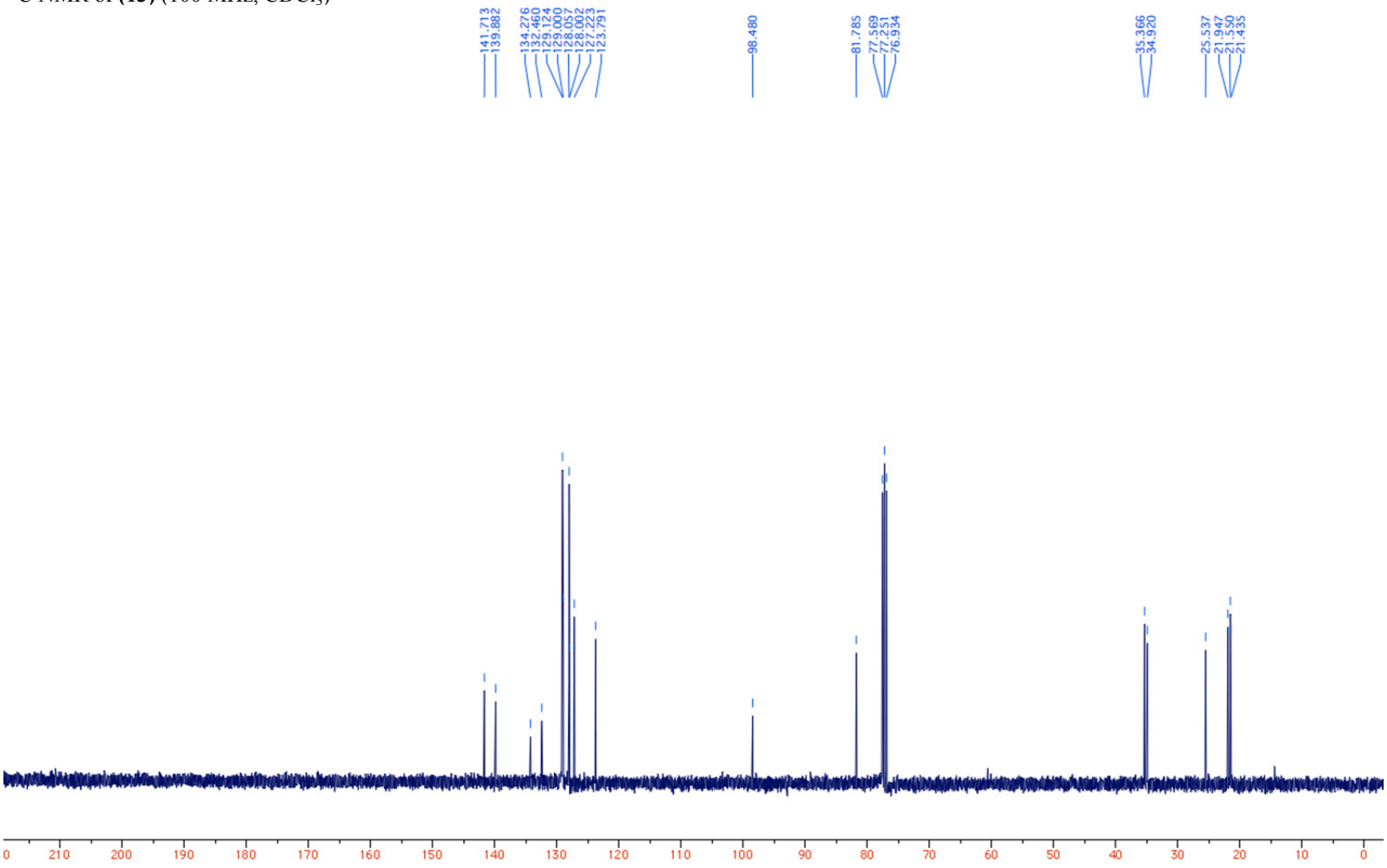

^{1}H NMR of **(14)** (400 MHz, $CDCl_3$)

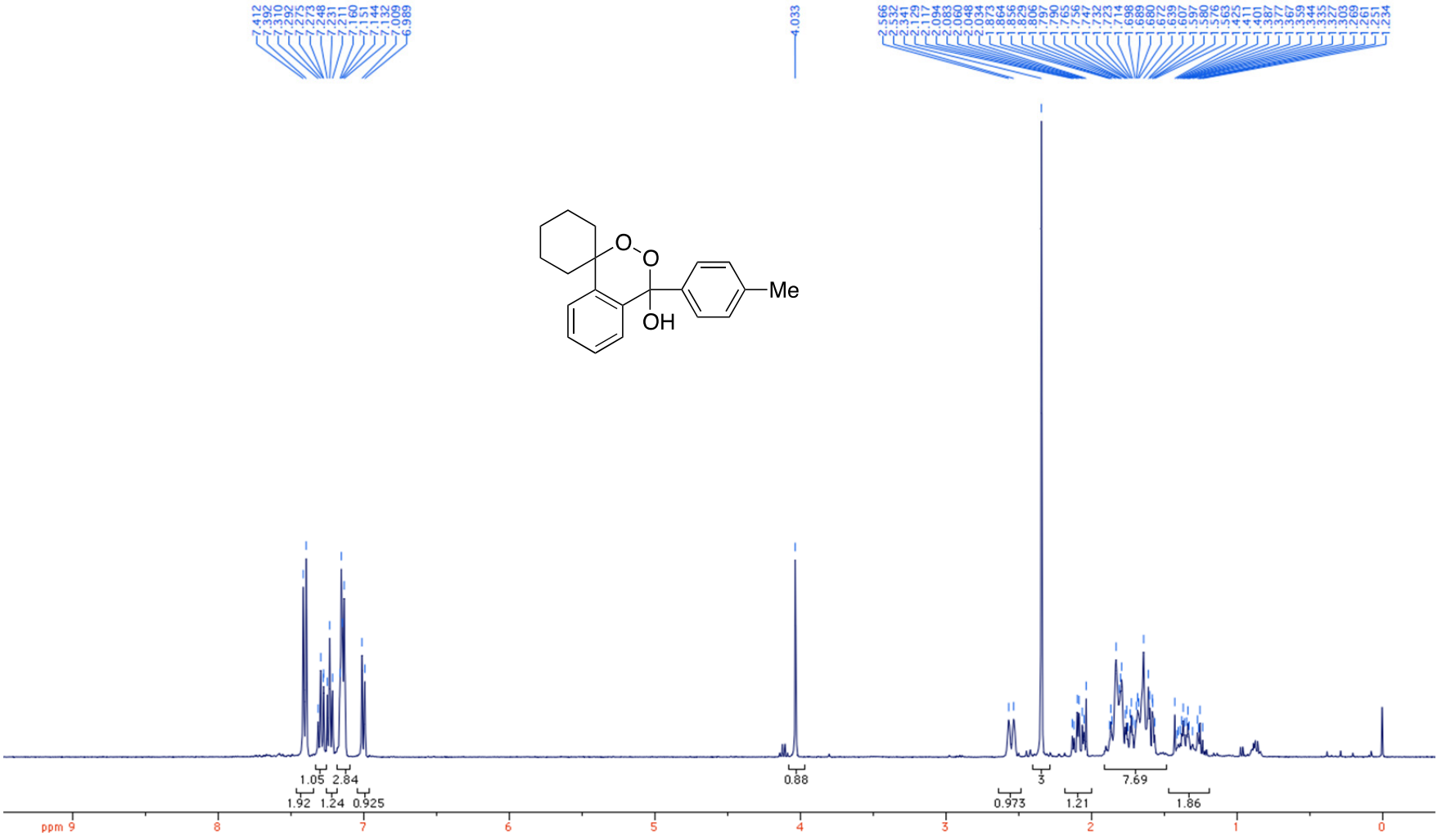

^{13}C NMR of **(14)** (100 MHz, $CDCl_3$)

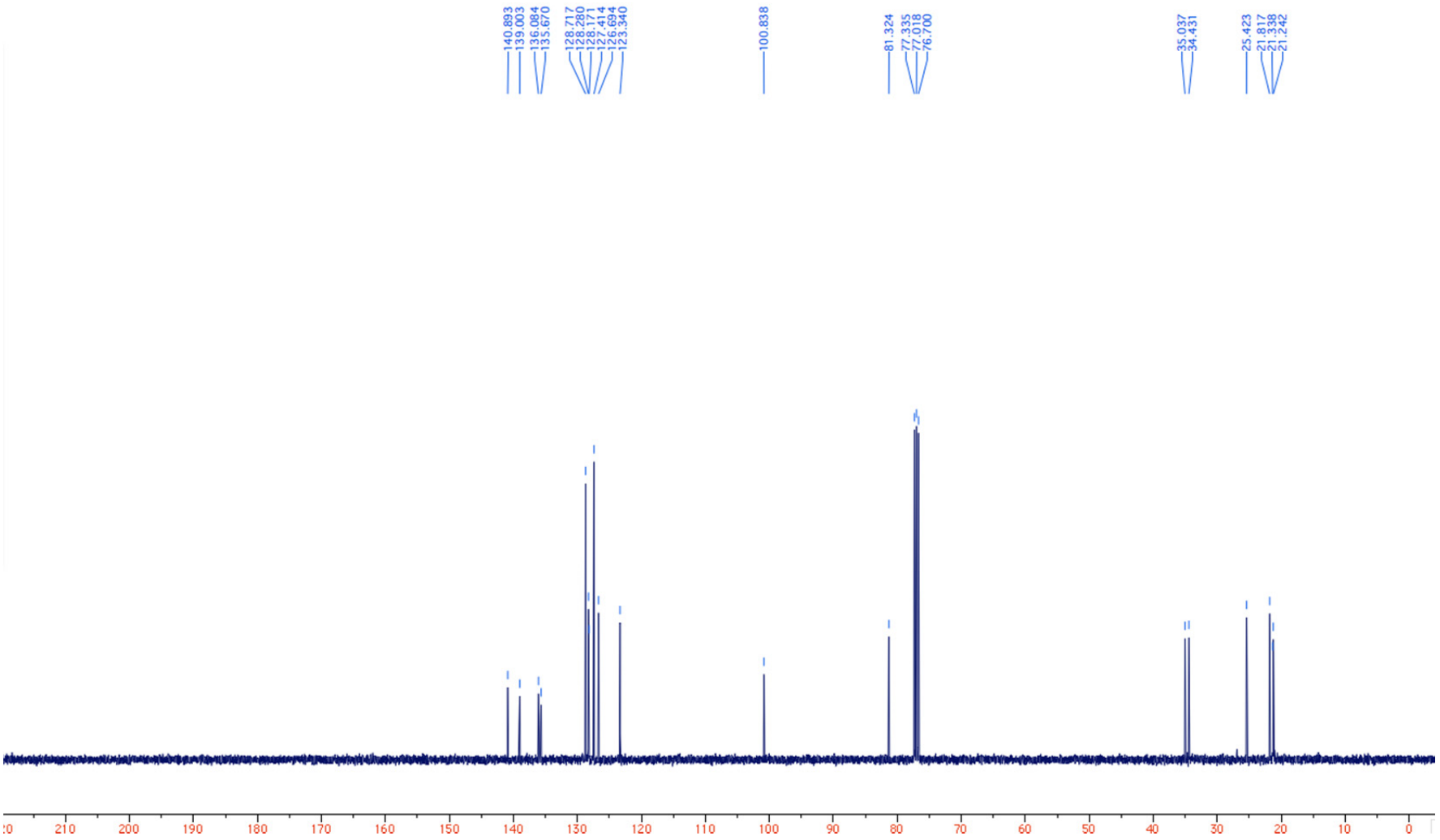

^{1}H NMR of **(15)** (400 MHz, $CDCl_3$)

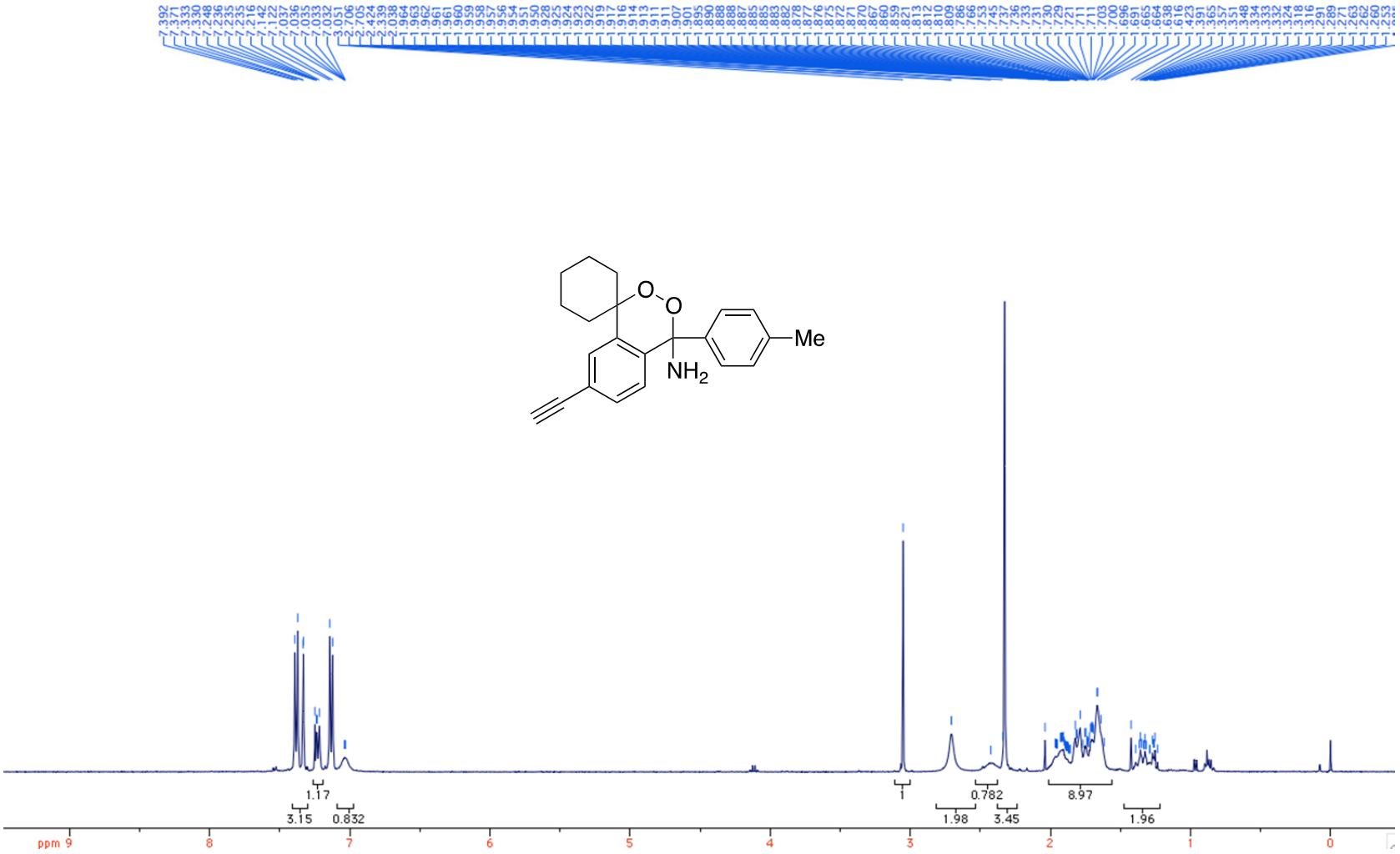

^{13}C NMR of **(15)** (100 MHz, $CDCl_3$)

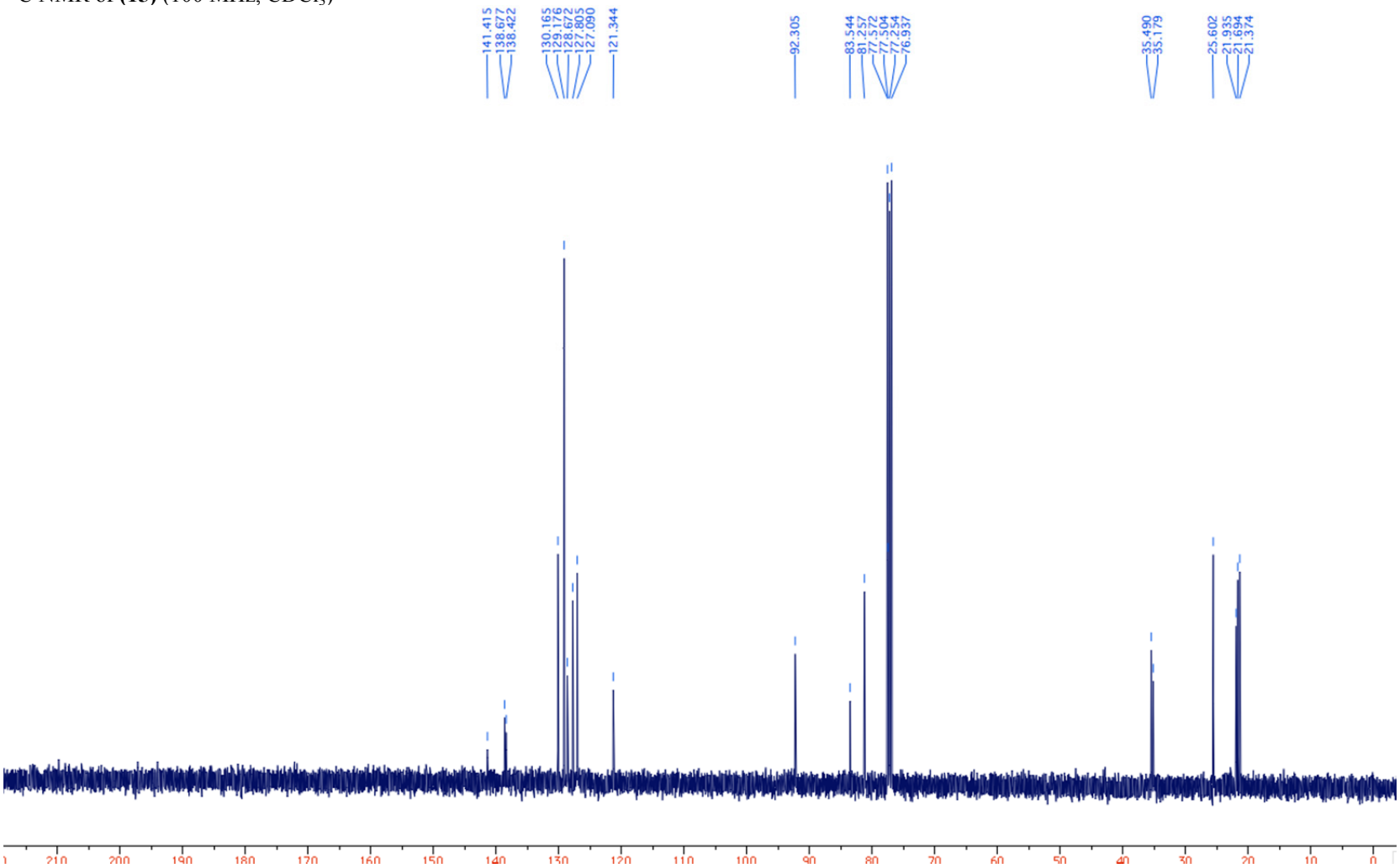

^{1}H NMR of starting material for **(15)** (400 MHz, $CDCl_3$)

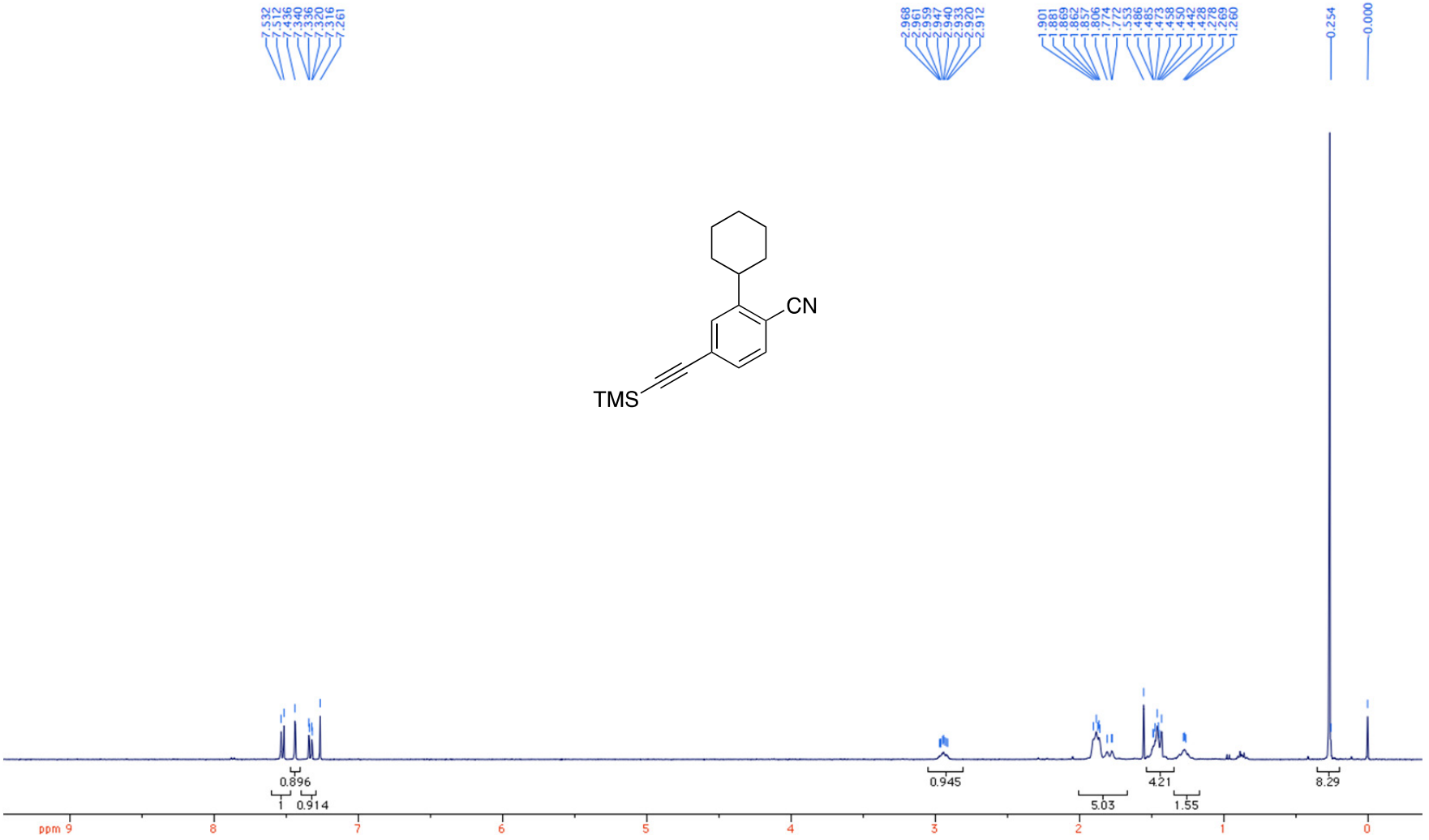

^{13}C NMR of starting material for **(15)** (100 MHz, $CDCl_3$)

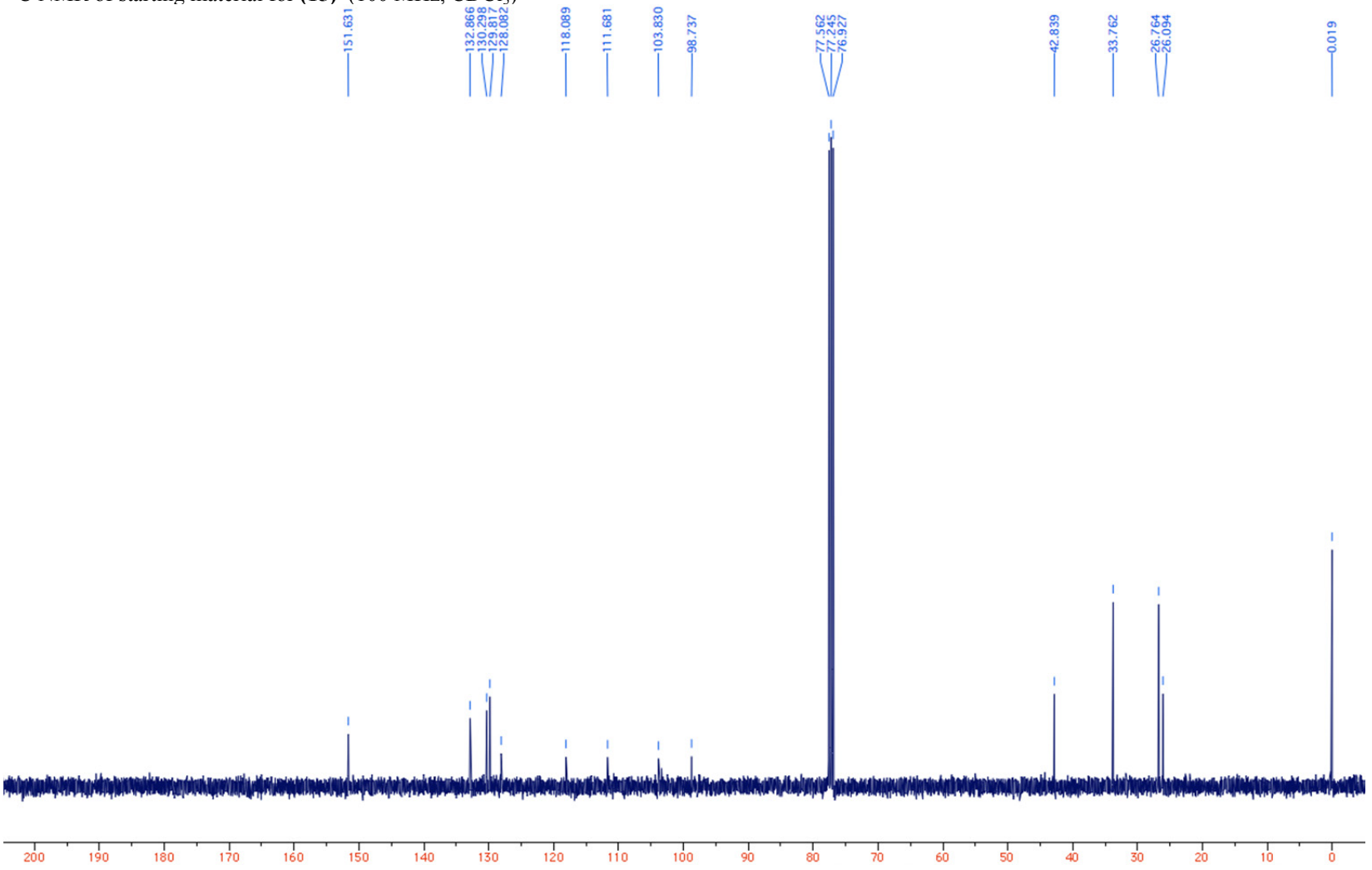

Supplementary Figures

Supplementary Figure S1. Series of naturally occurring endoperoxides exhibiting potent activities as anti-malaria and anti-cancer agents.

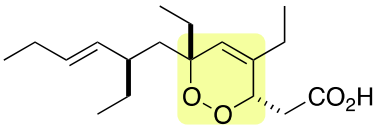

Haterumadioxin A
(cytotoxicity
against 38 human cancer cell lines)

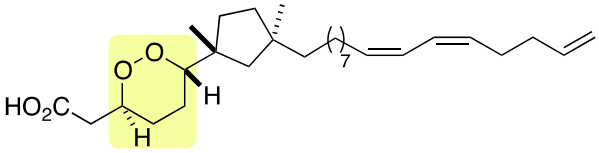

Stolonic Acids A
(antiproliferative acticity against
human melanoma and ovarian tumor cell lines)

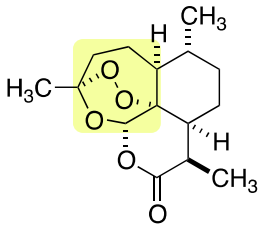

Qinghaosu (Artemisinin)
(antimalarial activity)

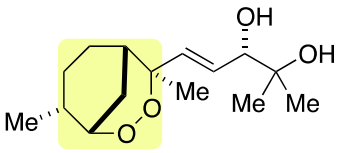

Yingzhaosu A
(antimalarial activity)

Supplementary Figure S2. Amino endoperoxides and derivatives selectively cause cancer cells to undergo apoptosis.

(A-D) FACS graphs on Annexin V and propidium iodide (PI) staining assays done on cells of: (A and C) Adherent and suspension MDA-MB-231 cells induced by treatment with indicated amino endoperoxide compounds under indicated concentrations for 0.5 h; (B) adherent and suspension MCF-10A cells induced by treatment with indicated amino endoperoxide compounds under 500 μM concentrations for 0.5 h; (D) suspension MDA-MB-231 cells induced by treatment with 4-Me with 1uM for indicated times as analysed by FACS (5000 events). (E) Percentage of Annexin V positive (apoptotic) cells calculated based on (D). Error bars: s.e.m. ***$p<0.001$.

Vehicle-treated cells served as cognate controls for comparison. The sum of Annexin V^+/PI^- (early apoptosis) and Annexin V^+/PI^+ (late apoptosis) cells were considered apoptotic. Values (bold) denote apoptotic cells (%). Results are representative of three independent experiments. All experiments were performed three or four times with consistent results.

Supplementary Figure S2

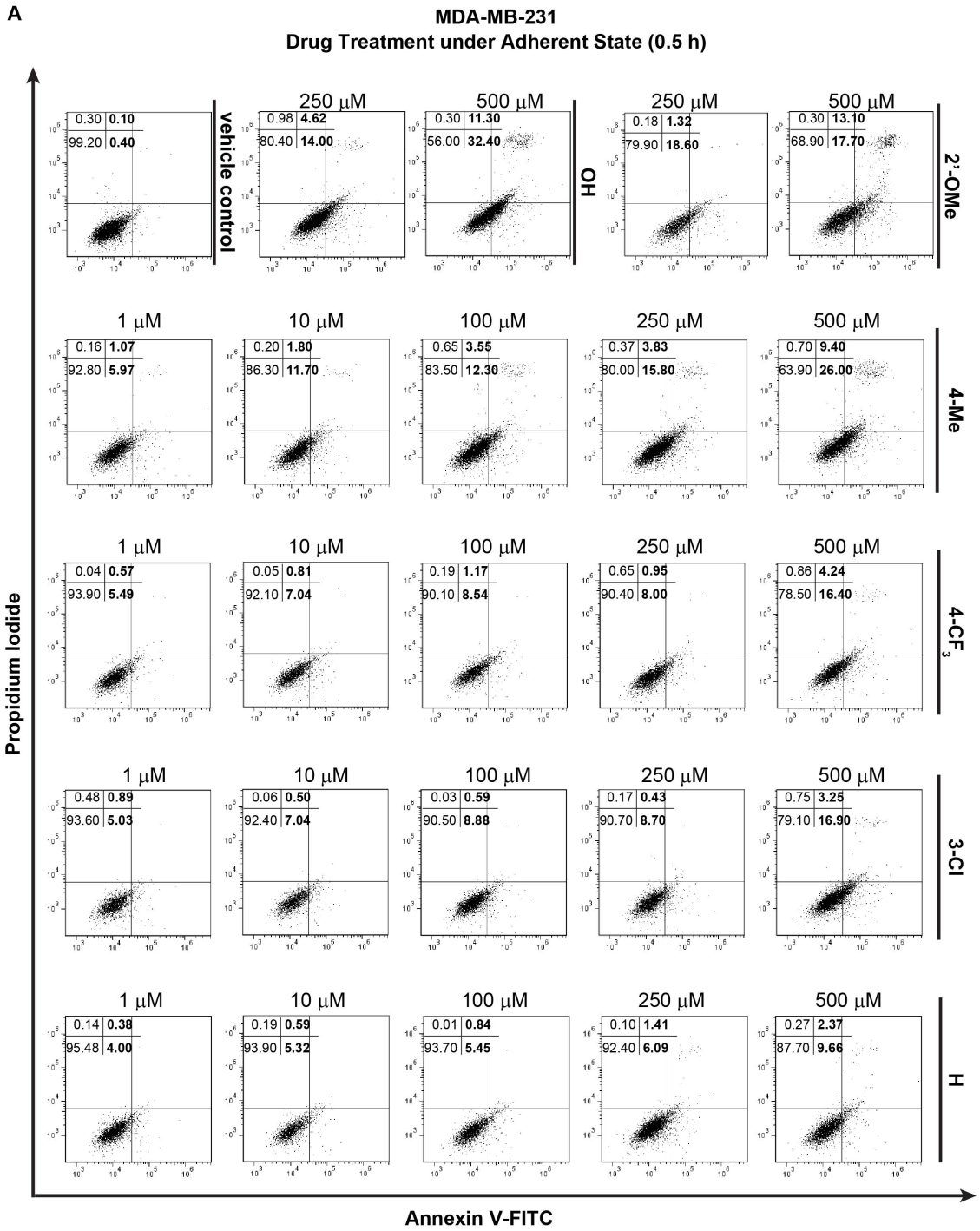

Supplementary Figure S2

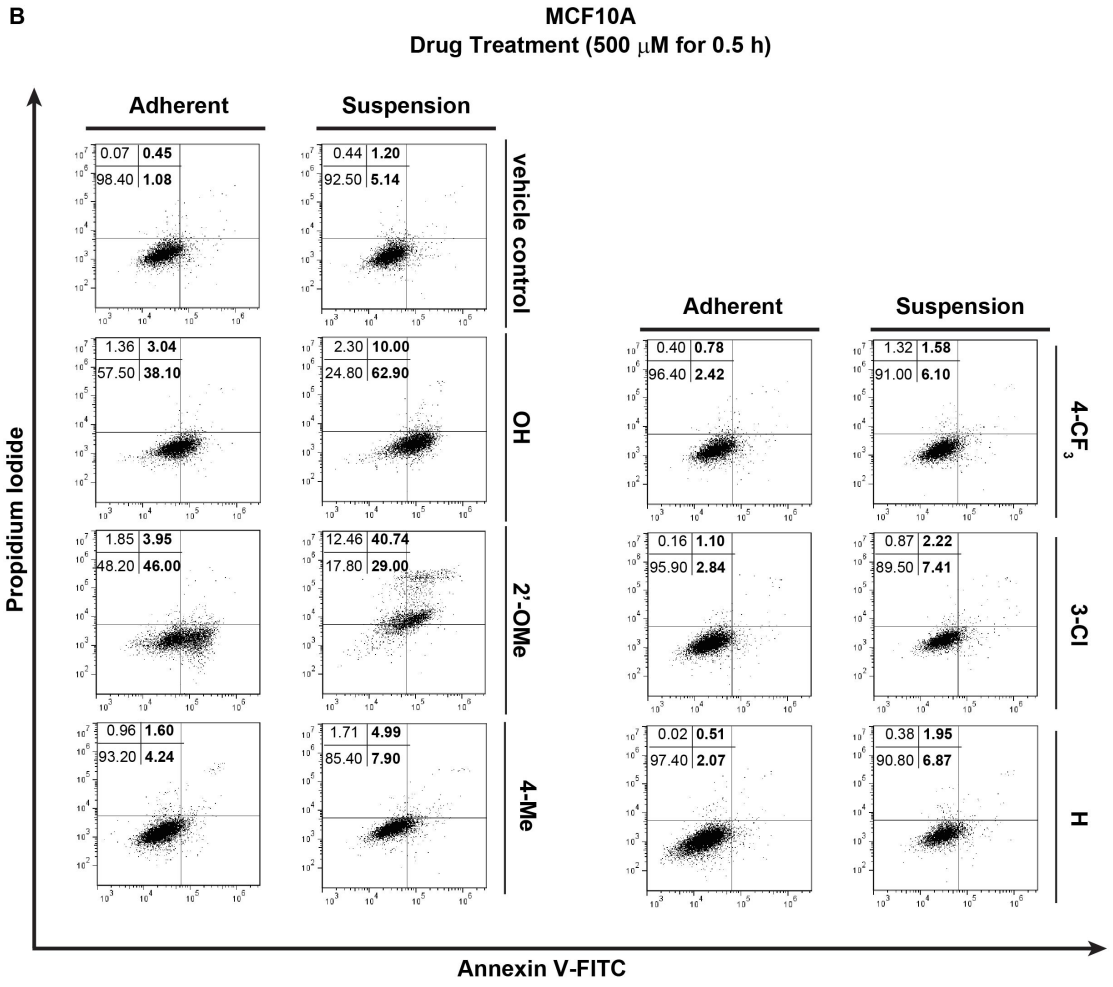

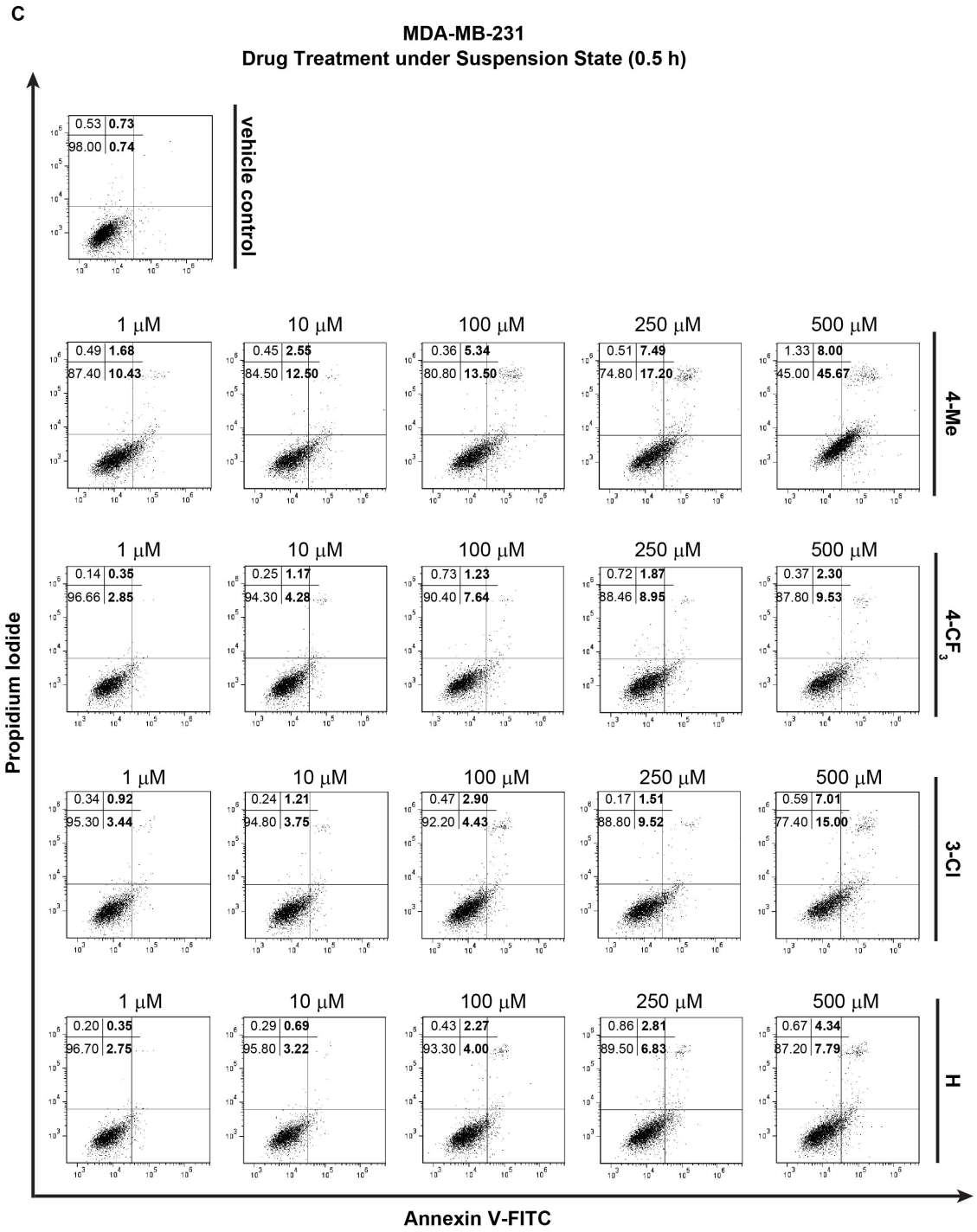
C
MDA-MB-231
Drug Treatment under Suspension State (0.5 h)
vehicle control
0.53 0.73
98.00 0.74
1 μM
10 μM
100 μM
250 μM
500 μM
4-Me
0.49 1.68
87.40 10.43
0.45 2.55
84.50 12.50
0.36 5.34
80.80 13.50
0.51 7.49
74.80 17.20
1.33 8.00
45.00 45.67
4-CF3
0.14 0.35
96.66 2.85
0.25 1.17
94.30 4.28
0.73 1.23
90.40 7.64
0.72 1.87
88.46 8.95
0.37 2.30
87.80 9.53
3-Cl
0.34 0.92
95.30 3.44
0.24 1.21
94.80 3.75
0.47 2.90
92.20 4.43
0.17 1.51
88.80 9.52
0.59 7.01
77.40 15.00
H
0.20 0.35
96.70 2.75
0.29 0.69
95.80 3.22
0.43 2.27
93.30 4.00
0.86 2.81
89.50 6.83
0.67 4.34
87.20 7.79
Propidium Iodide
Annexin V-FITC

Supplementary Figure S2

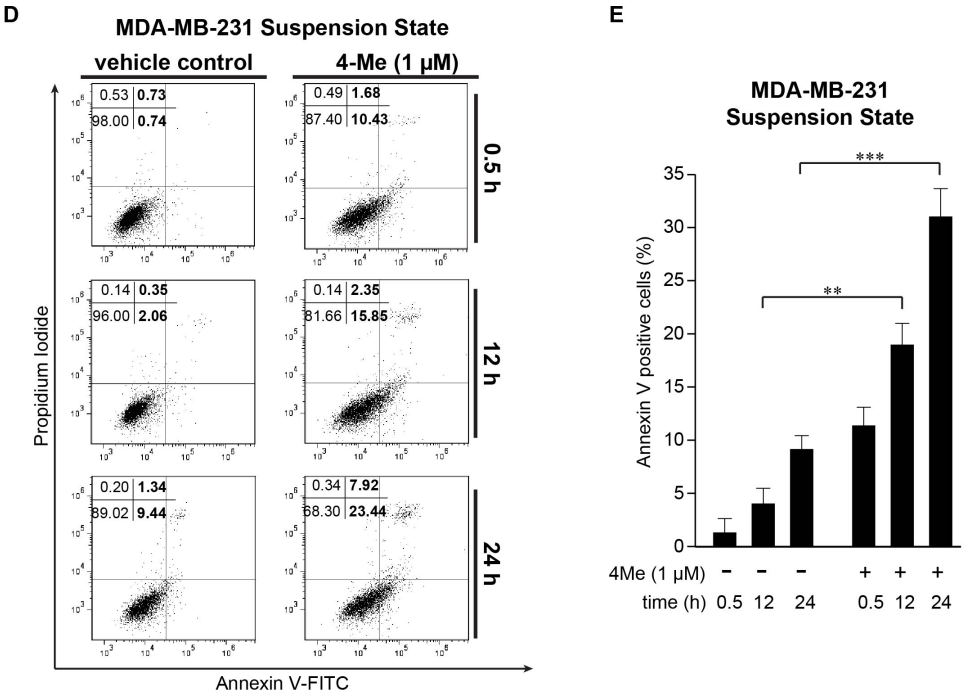

Supplementary Figure S3. 4-Me targets Nox4 to cause cell death.
(**A**) Amino acid sequence of full length human Nox4 protein. Peptide sequence underlined by various blue color lines shows LC-MS/MS (refer to Methods) results, indicating Nox4 as a potential target of 4-Me.
(**B**) cDNA encoding for the various truncated Nox4 were constructed using site-mutagenesis and subcloning into mammalian expression vector. Recombinant proteins were purified via nickel-affinity chromatography from lysate of transfected HEK293T cells. Representative Coomassie-stained gel and immunblot using anti-histidine tag antibody were shown. Lysate of untransfected (U) and transfected (T) cells served as negative and positive controls, respectively. Solutions with increasing concentrations of imidazole (1^{st}, 2^{nd} and 3^{rd}) were used to wash and eluted the bound proteins
(**C**) Relative mRNA and protein levels of Nox4 in MDA-MB-231 control and MDA-MB-231 Nox4 siRNA cells. The mRNA data (means± SD) are from two independent qPCR experiments performed in triplicates. The ribosomal protein 18S gene serves as a reference gene in qPCR and β-tubulin serves as a loading and transfer control in immunoblot.
(**D**) FACS graphs on Annexin V and propidium iodide (PI) staining assays done on various cells induced by treatment with 4-Me under indicated concentrations for 0.5 h as analysed by FACS (5000 events). Vehicle-treated cells served as cognate controls for comparison. The sum of Annexin V^+/PI^- (early apoptosis) and Annexin V^+/PI^+ (late apoptosis) cells were considered apoptotic. Values (bold) denote apoptotic cells (%). Results are representative of three independent experiments. All experiments were performed three or four times with consistent results.
(**E**) Representative sensogram of three independent experiments showing binding profile between immobilized-COX2 and 500 nM of 4-Me. Anti-COX2 antibody served as positive control. Sensograms were corrected against a reference flow cells with no immobilised proteins.

Supplementary Figure S3

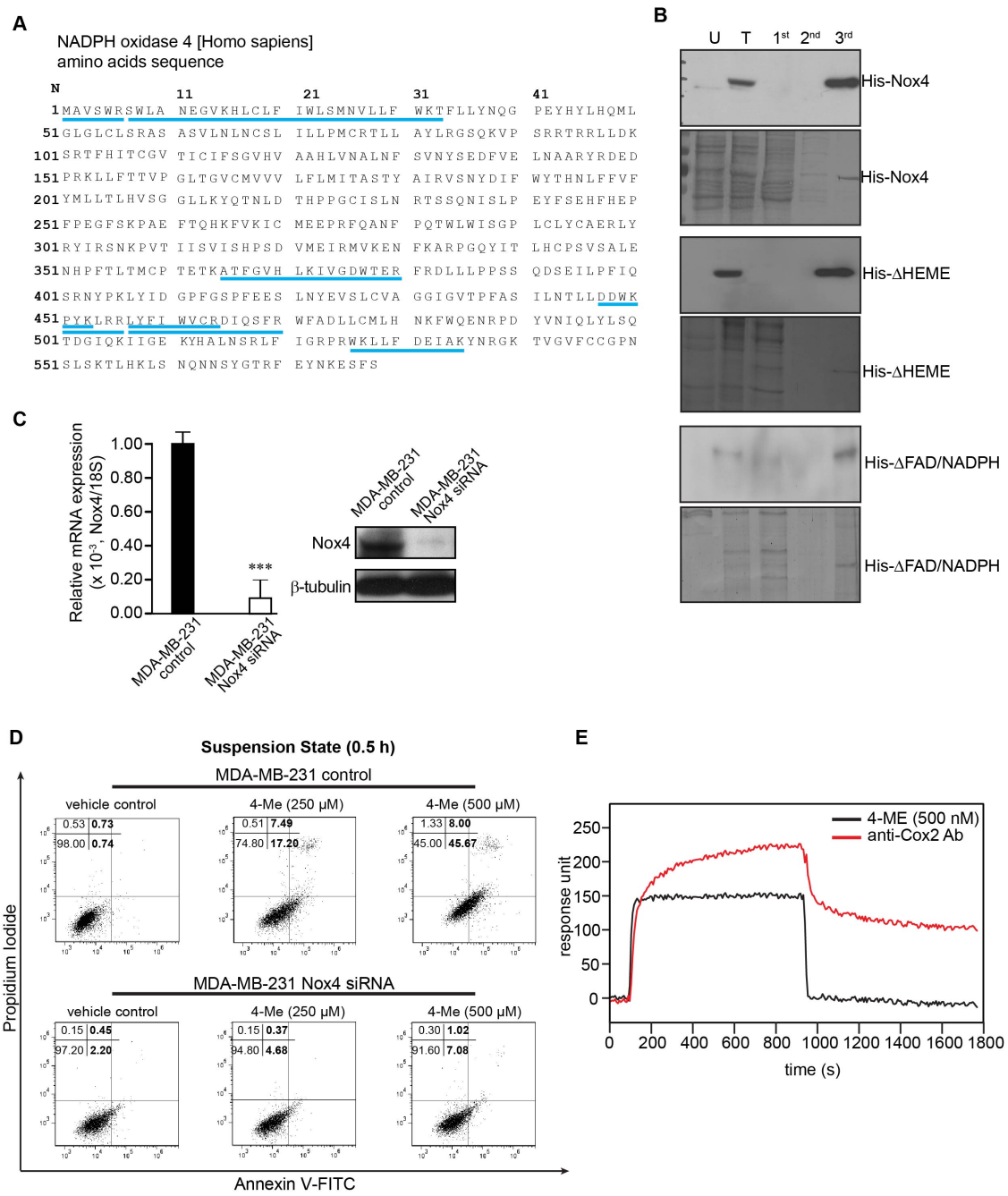

Supplementary Figure S4. 4-Me causes Nox4 overexpressed HEK 293T cells to undergo apoptosis.

(A) and **(C)** Percentage of Annexin V positive stained A-5RT3 (A) and Nox4-transfected HEK 293T cells (C) that of 0.5 h treatment of 500 μM 4-Me as analysed by FACS (5000 events). Vehicle-treated cells served as control. The sum of Annexin V^+/PI^- (early apoptosis) and Annexin V^+/PI^+ (late apoptosis) cells were considered apoptotic. Values (bold) denote apoptotic cells (%). Results are representative of three independent experiments.

(B) Immunoblot of indicated antibodies on total cell lysates of control and Nox4-transfected HEK 293T cells. Immunoblot data are from three independent experiments performed in duplicate. β-tubulin serves as a loading and transfer control.

Supplementary Figure S4

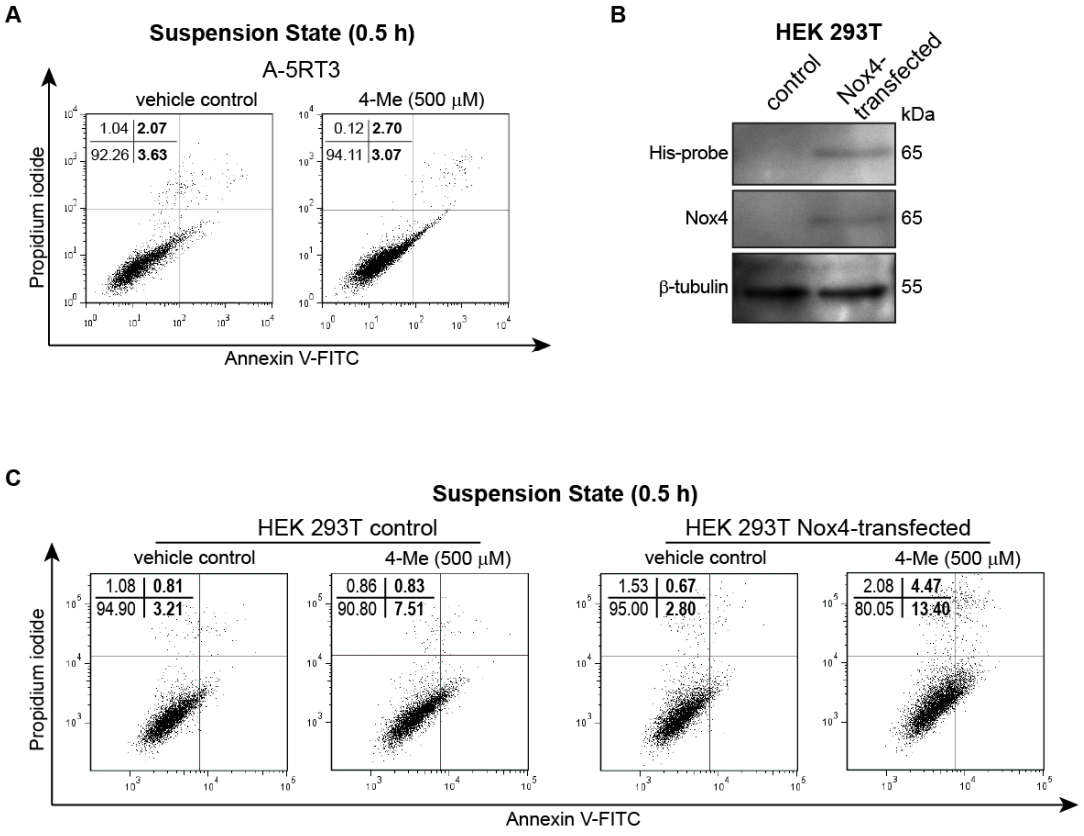

Supplementary Figure S5. 4-Me induces apoptosis and DNA damage on breast cancer cells but has no effect on their cell cycle.

(**A**) Immunoblots of DNA damage and apoptotic markers (cleaved PARP and cleaved caspase-3, respectively) on cell lysate of vehicle and indicated concentrations of 4-Me-treated MDA-MB-231 cells. Immunoblot data are from three independent experiments performed in duplicate. β-tubulin serves as a loading and transfer control.

(**B**) FACS graphs on cell cycle analysis using PI staining on suspension MDA-MB-231 cells under various treatments for 0.5 h. Percentage of various cell cycle phases in each sample conditions are shown. No significant change was observed between the various treatments. Results are representative of three independent experiments with triplicates.

(**C**) Percentage of Annexin V positive (apoptotic) cells calculated based on (A). Error bars: s.e.m. ***p<0.001.

(**D**) FACS graphs on Annexin V and propidium iodide (PI) staining assays done on suspension MDA-MB-231 cells induced by treatment either with 4-Me alone or in a combination of 4-Me and NAC under indicated concentrations for 0.5 h as analyzed by FACS (5000 events). The sum of Annexin V^+/PI^- (early apoptosis) and Annexin V^+/PI^+ (late apoptosis) cells were considered apoptotic. Values (bold) denote apoptotic cells (%). Results are representative of three independent experiments performed three or four times with consistent results.

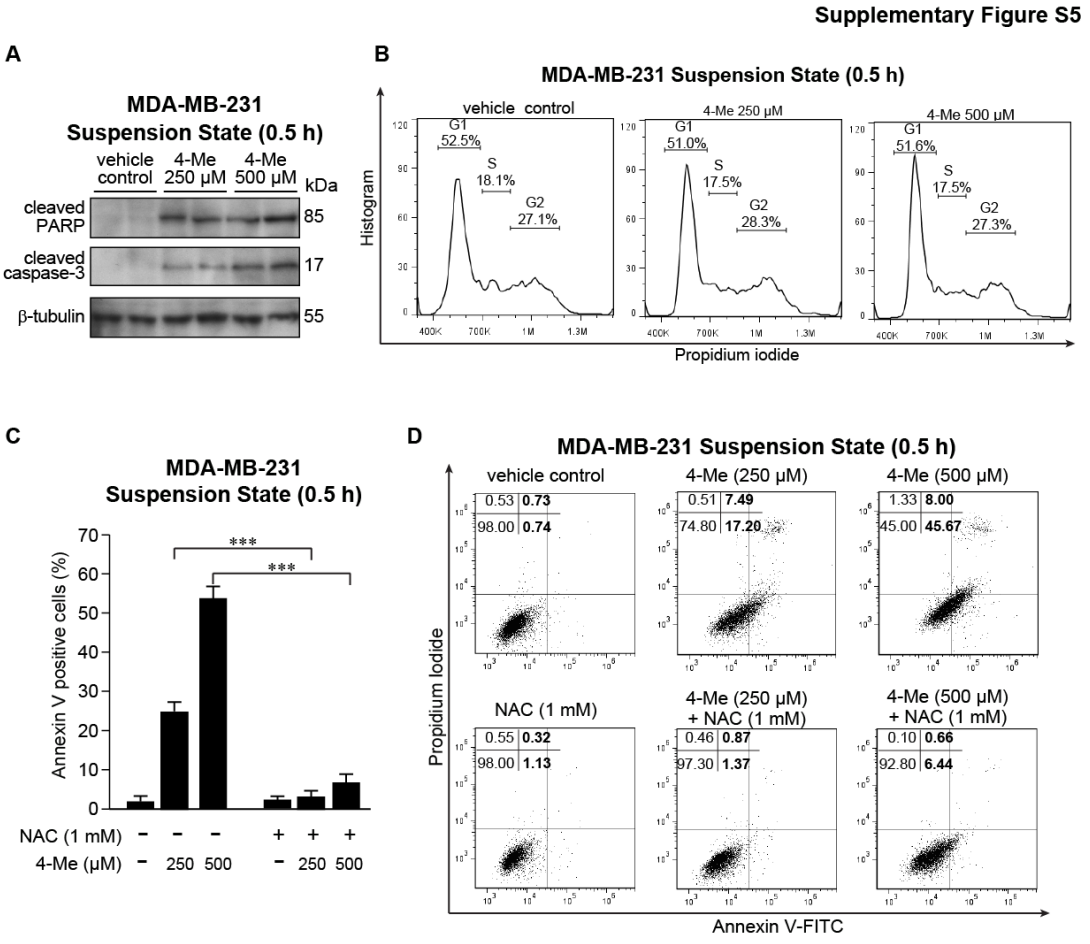

Supplementary Figure S6. Suppression of Nox4 abolishes the 4-Me effect on cellular ROS modulation.

(A) Representative FACS-derived histograms showing general ROS levels in suspension MDA-MB-231 control and MDA-MB-231 Nox4 siRNA cells in the presence of indicated concentrations 4-Me for 0.5 h as measured by CM-H2DCFDA.

(**B**) Relative fold change in general ROS level (mean DCF fluorescence intensities) as calculated from result of (A).

(**C-D**) H_2O_2 (C) and O_2^- (D) levels in suspension MDA-MB-231 control and MDA-MB-231 Nox4 siRNA cells in the presence of 4-Me under indicated concentrations for 0.5 h as determined by Amplex Red and MCLA assays, respectively.

(**E**) Arbitrary relative O_2^-:H_2O_2 ratios calculated based on H_2O_2 (C) and O_2^- (D) values are shown in the box.

(**F**) Levels of ·OH (expressed as fold change) in suspension MDA-MB-231 control and MDA-MB-231 Nox4 siRNA cells in the presence of 4-Me under indicated concentrations for 0.5 h measured using terephthalic acid. The ·OH quencher dimethylthiourea (DMTU) was used as the negative control.

Each experiment was independently performed two to three times with triplicates. The value of cognate vehicle controls was set as 1. Error bars, s.e.m. n.s. represents not significant, * $p < 0.05$, **$p<0.01$.

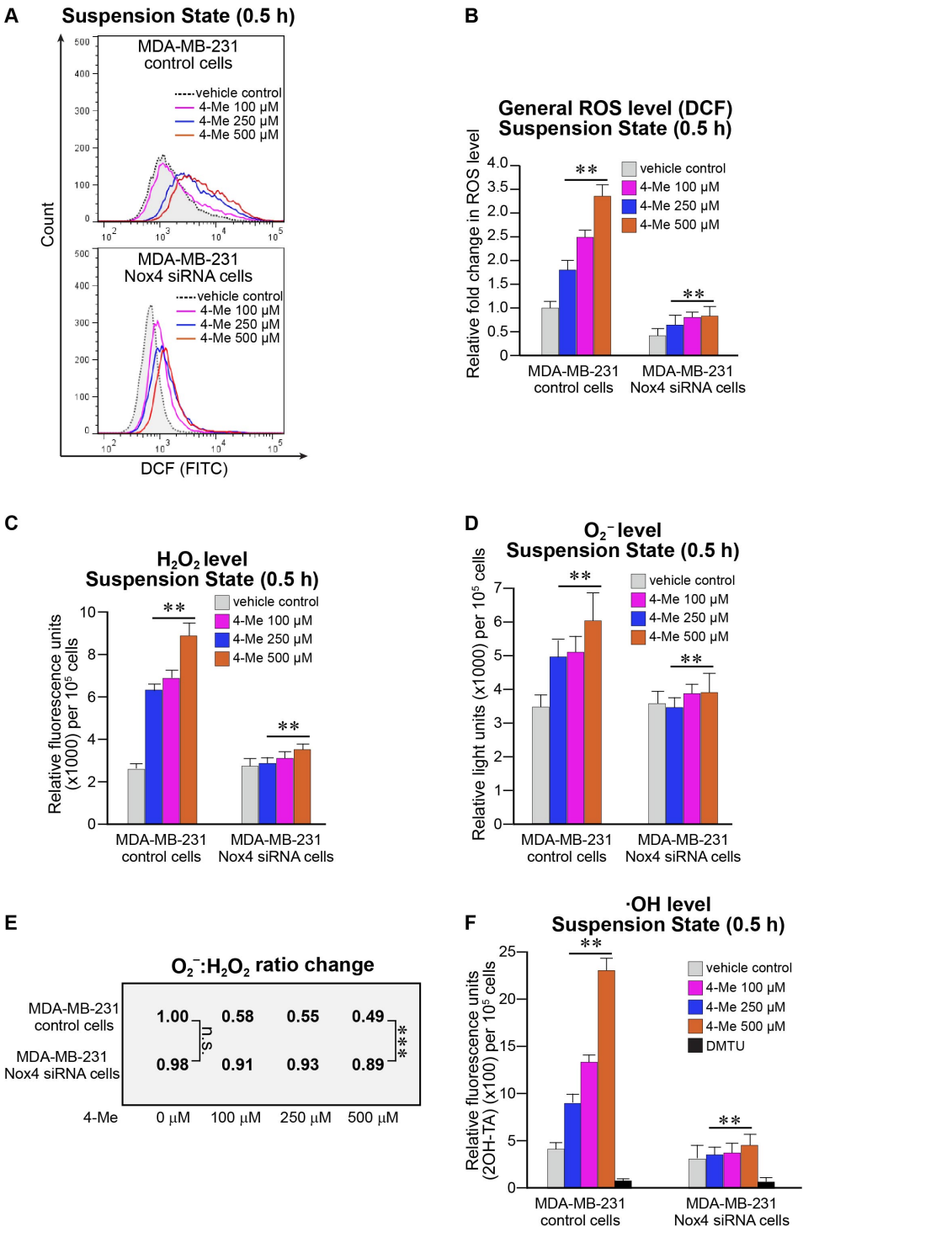
A
Suspension State (0.5 h)
MDA-MB-231
control cells
vehicle control
4-Me 100 μM
4-Me 250 μM
4-Me 500 μM
MDA-MB-231
Nox4 siRNA cells
Count
DCF (FITC)
B
General ROS level (DCF)
Suspension State (0.5 h)
Relative fold change in ROS level
MDA-MB-231
control cells
MDA-MB-231
Nox4 siRNA cells
C
H2O2 level
Suspension State (0.5 h)
Relative fluorescence units
(x1000) per 10^5 cells
D
O2− level
Suspension State (0.5 h)
Relative light units (x1000) per 10^5 cells
E
O2−:H2O2 ratio change
MDA-MB-231
control cells
MDA-MB-231
Nox4 siRNA cells
1.00
0.58
0.55
0.49
0.98
0.91
0.93
0.89
n.s.
***
4-Me
0 μM
100 μM
250 μM
500 μM
F
·OH level
Suspension State (0.5 h)
Relative fluorescence units
(2OH-TA) (x100) per 10^5 cells
DMTU

Supplementary Figure S7. High dosages of 4-Me shows little drug-related toxicity on the liver, kidney and heart.
(A) Haematoxylin and eosin staining of liver, kidney and heart sections from mice treated with 51.5 µmol/kg and 103 µmol/kg of 4-Me-treated mice.
(B) Immunblot analysis of caspase 3 in indicated tissues. Antibodies against caspase 3 detected both the full-length and cleaved forms.

Supplementary Figure S7

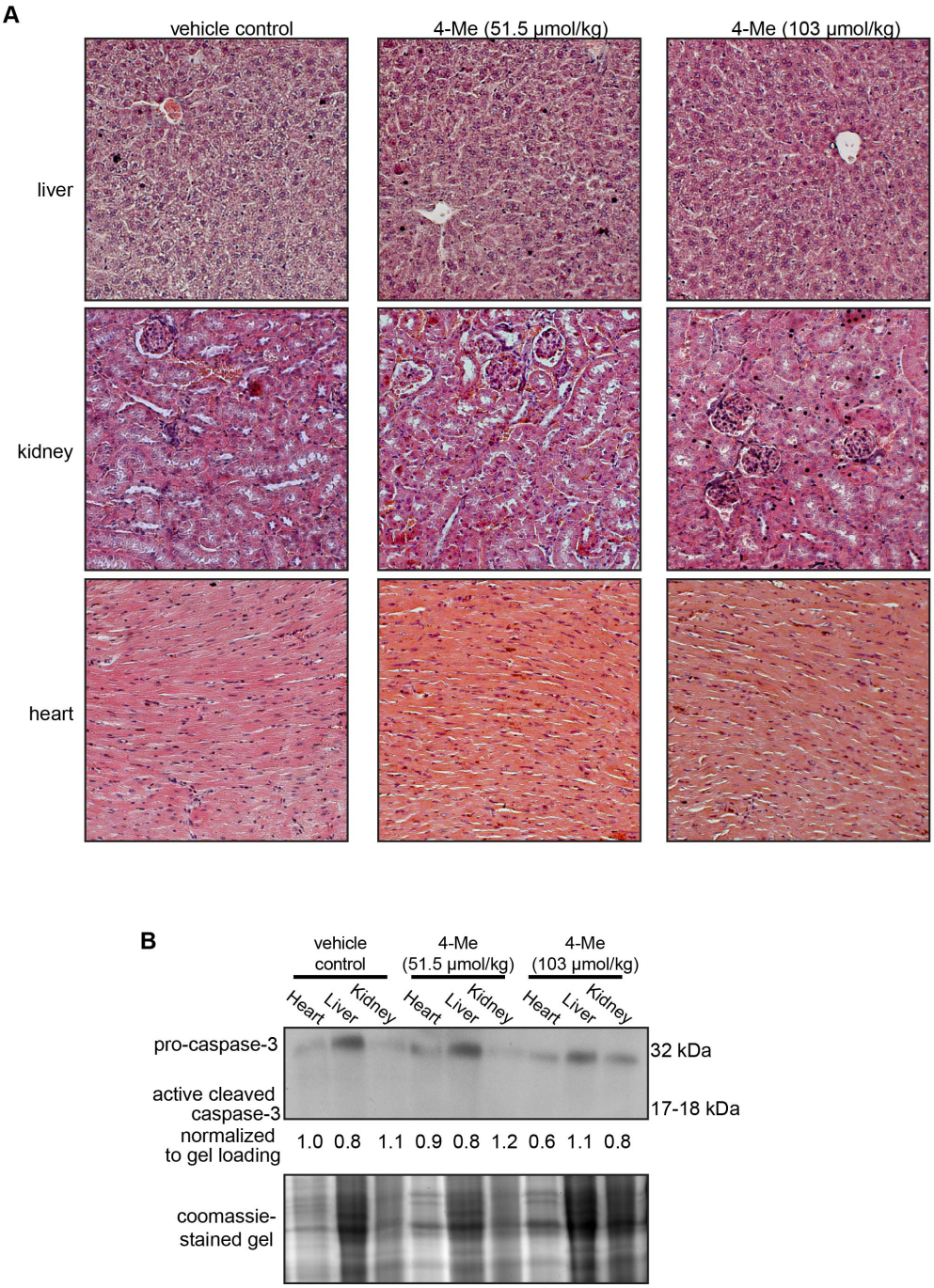

Supplementary Methods

H&E and immunofluorescence assay

Mouse tumor biopsies were fixed with 4% paraformaldehyde and subsequently frozen in Tissue-Tek OCT compound medium (Sakura) at -70 ºC for cryosectioning. Crysostat sections (8 μm) were processed for Haematoxylin (H) & Eosin (E) and immunofluorescence study. For H&E staining, tissue sections were stained with H for 5 min, followed by a 2 sec rinse in 1% HCl and a 3 min development under running water, and finally a 27 sec staining with E. For Ki67 staining, Alexa Fluor 488-conjugated goat anti-mouse secondary antibody was used. Apoptotic tumor cells were detected using the TUNEL assay according to the manufacturer's protocol (Roche). As positive control for TUNEL assay, the section was pretreated with DNase I. The slides were mounted with antifade reagent (ProLong Gold; Invitrogen) with DAPI. Images were acquired in one z-plane using a LSM710 confocal laser scanning microscope and ZEN 2008 software (Carl Zeiss).

Transfection in HEK 293T cells

Mammalian expression plasmids containing the cDNA sequences encoding human full-length Nox4 (WT), the heme (ΔFAD/NADPH) or NADPH (ΔHEME) region with N-terminal histidine tag were transfected into HEK 293T cells using FuGENE®HD (Promega) following manufacturer's protocol. An empty plasmid vector was used as control. Transfected cells were lysed in lysis buffer (300 mM NaCl, 50 mM Tris.HCl, pH8.0, 0.1% Triton-X). Recombinant WT, ΔFAD/NADPH and ΔHEME Nox4 proteins were affinity purified using Ni-NTA and verified using anti-His antibody (Santa Cruz

Biotechnology). Purified recombinant proteins were dialyzed against 100 mM NaCl, 20 mM HEPES, pH 8.0 before surface plasmon resonance analysis. Nox4-expressing HEK293 cells were also used for amino endoperoxide treatment assay.

Total RNA isolation and quantitative real-time PCR (qPCR)

Total RNA was extracted and qPCR was performed as previously described.[7] Expression was normalized to the housekeeping gene 18S ribosomal protein. The primer sequences were: Nox4 sense (5' GCT GAC GTT GCA TGT TTC AG 3'); Nox4 antisense (5' CGG GAG GGT GGG TAT CTA A 3'); 18S sense (5' GTA ACC CGT TGA ACC CCA TT 3'); 18S antisense (5' CCA TCC AAT CGG TAG TAG CG 3').

Cell cycle analysis

Cells were suspended for 0.5 h in the presence of various concentrations of 4-Me. Next, cells were harvested and washed twice with PBS, followed by ethanol fixation at 4 ºC overnight. The next day, cells were washed with PBS and stained for propidium iodide in the presence of 50 mM of RNase A at 37 ºC for 1 h. Samples were washed and resuspended with PBS before being subjected to FACS analysis.

Surface Plasmon Resonance (SPR)

SPR analyses were performed as previously described[8,9] with minor modifications. Purified recombinant human Nox4 deletion mutants (FL-full length Nox4, ΔFAD/NADPH- Nox4 deleted of FAD/NADPH regions and ΔHEME- Nox4 deleted of

HEME region) were immobilised onto CM5 Sensorchip by amine coupling (GE Healthcare). PBS was used as running buffer.

References

1. Shi Z, Zhang C, Tang C, Jiao N. Recent advances in transition-metal catalyzed reactions using molecular oxygen as the oxidant. *Chem Soc Rev* 2012; **41:** 3381-3430.
2. Wendlandt A E, Suess AM, Stahl SS. Copper-catalyzed aerobic oxidative C-H functionalizations: trends and mechanistic insights. *Angew Chem Int Ed Engl* 2011; **50:** 11062-11087.
3. Zhang L, Ang GY, Chiba S. Copper-catalyzed benzylic C-H oxygenation under an oxygen atmosphere via N-H imines as an intramolecular directing group. *Org Lett* 2011; **13:** 1622-1625.
4. Cahiez G, Lepifre F, Ramiandrasoa P. Manganese-Catalyzed Substitution of activated Aryl Halides (X = Cl, Br and F) and Aryl Ethers by Organomagnesium Reagents. *Synthesis* 1999; 2138-2144.
5. Schareina T, Zapf A, Mägerlein W, Müller N, Beller M. A state-of-the-art cyanation of aryl bromides: a novel and versatile copper catalyst system inspired by Nature. *Chem Eur J* 2007; **13:** 6249-6254.
6. Tran LD, Daugulis O. Iron-catalyzed heterocycle and arene deprotonative alkylation. *Org Lett* 2010; **12:** 4277-4779.
7. Chong HC, Tan MJ, Philippe V, Tan SH, Tan CK, Ku CW. Regulation of epithelial-mesenchymal IL-1 signaling by PPARbeta/delta is essential for skin homeostasis and wound healing. *J Cell Biol* 2009; **184:** 817-831.

8. Zhu P, Tan MJ, Huang RL, Tan CK, Chong HC, Pal M *et al.* Angiopoietin-like 4 protein elevates the prosurvival intracellular O2(-):H2O2 ratio and confers anoikis resistance to tumors. *Cancer Cell* 2011; **19:** 401-415.
9. Goh YY, Pal M, Chong HC, Zhu P, Tan MJ, Punugu L. Angiopoietin-like 4 interacts with integrins beta1 and beta5 to modulate keratinocyte migration. *Am J Pathol* 2010; **177:** 2791-2803.